Electronic Supplementary Material (ESI) for ChemComm.

Supplementary Information

Bis(amidinate) Ligands in Early Lanthanide Chemistry – Synthesis, Structures, and Hydroamination Catalysis

Neda Kazeminejad,[a] Denise Girnt,[a] Michael T. Gamer,[a] and Peter W. Roesky*[a]

[a]: Institute of Inorganic Chemistry Karlsruhe Institute of Technology (KIT), Engesserstraße 15, 76131 Karlsruhe (Germany).

EXPERIMENTAL SECTION

Synthesis

General methods. All air- and water-sensitive materials were prepared under an argon atmosphere on a Schlenk line or in a glovebox. THF was distilled from potassium metal under nitrogen before use. Toluene, *n*-heptane and *n*-pentane were dried using an M. Braun solvent purification system (SPS-800). Deuterated solvents were purchased from Aldrich GmbH (99 atom % D) and were dried, and stored under vacuum with Na/K alloy. All other chemicals were purchased and used without further purification. NMR spectra were recorded on a Bruker Avance II 300 MHz or Avance III 400 MHz NMR spectrometer. Elemental analyses were carried out on an Elementar Vario mirco cube. IR spectra were performed on a Bruker TENSOR 37 spectrometer via the attenuated total reflection method (ATR). $[La\{N(SiMe_3)_2\}_3]$ and $[Sm\{N(SiMe_3)_2\}_3]$ were prepared using a modified procedure of Bradley et. al.[1] We found that using 2.90 equivalents of $K\{N(SiMe_3)_2\}$ instead of 3 equivalents $Li\{N(SiMe_3)_2\}$ gave good yields without the formation of 'ate' complexes or the need for added purification.

Synthesis of ${}^{\mathbf{p\text{-}Tolyl}}\mathbf{L}_{\mathbf{DBF}}\mathbf{H}_2$:

8 mL of 2.5 M *n*-BuLi in *n*-hexane (20.0 mmol) were added to a solution of dibenzofurane (1.43 g, 8.5 mmol) and TMEDA (3.0 mL, 20.0 mmol) in 50 mL *n*-heptane. The suspension was stirred under reflux for 6 h. 1,3-Di-*p*-tolylcarbodiimide (4.10 g, 18.4 mmol) in 100 ml *n*-heptane was added at room temperature to the reaction mixture. The suspension was hydrolyzed after stirring for 18 hours at r.t. The precipitation was filtered, washed with water and *n*-pentane, and dried under vacuum, giving ${}^{p\text{-}Tolyl}L_{DBF}H_2$ as a white powder. Single crystals suitable for single crystal X-ray diffraction were obtained from dimethylsulfoxide (DMSO) at room temperature. Yield: 2.76 g (53 %). ${}^1H$ NMR (d_6-DMSO, 400 MHz, 25 °C): δ = 2.03 (br s, 6H, CH_3), 2.26 (br s, 6H, CH_3), 6.47 (br s, 4H, *Ar*), 6.66 (br s, 4H, *Ar*), 7.07 (br s, 4H, *Ar*), 7.30 (t, ${}^3J_{H,H}$ = 7.6 Hz, 2H, *Ar*), 7.39 (d, ${}^3J_{H,H}$ = 7.4 Hz, 2H, *Ar*), 7.77 (br s, 4H, *Ar*), 8.04 (d, ${}^3J_{H,H}$ = 7.6 Hz, 2H, *Ar*), 9.12 (br s, 2H, N*H*) ppm. ${}^{13}C\{{}^1H\}$-NMR (d_6-DMSO, 75 MHz, 25 °C): δ = 20.4 (CH_3), 119.7 (*Ar*), 119.8 (*Ar*), 121.6 (*Ar*), 121.9 (*Ar*), 122.8 (*Ar*), 123.4 (*Ar*), 128.0 (*Ar*), 128.7 (*Ar*), 128.7 (*Ar*), 129.4 (*Ar*), 130.7 (*Ar*), 138.8 (*Ar*), 147.9 (*Ar*), 150.0 (*Ar*), 152.0 ($ArCN_2$) ppm. EI/MS (70 eV, 190 °C): m/z (%) = 612 (M^+, 80), 512 (M^+-(NH-C_6H_4-CH_3), 93), 401 (M^+-(N-C_6H_4-CH_3)$_2$, 20), 309 (M^+-(HN-C_6H_4-CH_3)$_2$-$C_6H_4CH_3$, 87), 283 (M^+-(HN-C_6H_4-CH_3)$_2$-$NC_6H_4CH_3$, 12). - IR (ATR) ($\tilde{\nu}$/cm^{-1}): 3376 (w), 3025 (w), 2963 (vs), 2913(w), 1626 (m), 1602 (m), 1509 (m), 1417 (m), 1373 (w), 1258 (s), 1220 (m), 1184 (m), 1085 (s), 1015 (vs), 859 (m), 792 (vs), 759 (s), 667 (m), 576 (w), 524 (m), 485(m). Elemental analysis calcd (%) for $[C_{42}H_{40}N_4O_3]$ (${}^{p\text{-}Tolyl}L_{DBF}H_2$ + $2H_2O$) (769.03): C 77.75, H 6.21, N 8.64; found C 77.84, H 5.40, N 8.98.

Synthesis of **($^{p\text{-Tolyl}}L_{DBF}K_2$)**

15 mL of THF was condensed onto a mixture of potassium bis(trimethylsilyl)amide (81.4 mg, 0.408 mmol) and $^{p\text{-Tolyl}}L_{DBF}H_2$ (100 mg, 0.163 mmol). The reaction mixture was stirred under reflux for four hours. After 15 minutes, gas evolution was observed and the suspension turned orange. The solvent was removed from the resulting precipitation under high vacuum and the residue was washed three times with *n*-pentane. The product was obtained as a bright orange powder. Yield: 97.2 mg (87 %). ^{1}H NMR (d_8-THF, 300 MHz, 25 °C): δ = 2.14 (s, 12H, *CH₃*), 6.81 (s, 8H, *Ar*), 7.02 (br s, 4H, *Ar*), 7.17 (t, $^3J_{H,H}$ = 7.6 Hz, 4H, *Ar*), 7.36 (d, $^3J_{H,H}$ = 7.68 Hz, 4H, *Ar*), 7.81 (d, $^3J_{H,H}$ = 8.6 Hz, 2H, Ar) ppm. ^{13}C{^{1}H} NMR (d_8-THF, 75 MHz, 25 °C): δ = 21.1 (CH_3), 121.8 (*Ar*), 121.9 (*Ar*), 122.1 (*Ar*), 122.2 (*Ar*), 122.7 (*Ar*), 123.3 (*Ar*), 125.0 (*Ar*), 129.1 (*Ar*), 129.5 (*Ar*), 130.6 (*Ar*), 153.9 ($ArCN_2$) ppm (some peaks overlap in the aromatic region). IR (ATR) ($\tilde{\nu}$/cm^{-1}): 2917 (w), 2862 (w), 1587 (m), 1472 (vs), 1448 (vs), 1411 (m), 1381 (s), 1252 (m), 1224 (m), 1139 (w), 1108 (w), 1056 (m), 967 (w), 926 (w), 882 (m), 830 (m), 813 (m), 791 (m), 761 (s), 718 (w), 665 (w), 598 (m), 526 (m), 485(s).

Synthesis of $[La_4(\mu\text{-}Cl)_4(^{p\text{-Tolyl}}L_{DBF})_4(THF)_4]$ (**1**).

Approximately 20 mL of THF was condensed onto a mixture of $^{p\text{-Tolyl}}L_{DBF}K_2$ (423 mg, 0.61 mmol) and $LaCl_3$ (335 mg, 1.37 mmol), and the suspension was stirred for 24 h at 65 °C. After 6 h, the bright orange suspension turned pale yellow. The solvent was then removed under high vacuum. The residue was dissolved in 15 mL of toluene, heated and then the warm solution was filtered. The solution was slowly cooled down to room temperature. After 5 h, small yellow crystals which were suitable for X-ray crystallography were obtained. Yield: 135 mg, (7 %). ^{1}H NMR (C_6D_6, 300 MHz, 25 °C): δ = 1.53 (s, 12H, *CH₃*), 1.88 (s, 12H, *CH₃*), 2.09 (s, 12H, *CH₃*), 2.38 (s, 12H, *CH₃*), 5.91 (d, $^3J_{H,H}$ = 8.1 Hz, 8H, *Ar*), 6.31 (d, $^3J_{H,H}$ = 8.6 Hz, 8H, *Ar*), 6.51 (d, $^3J_{H,H}$ = 8.1 Hz, 8H, *Ar*), 6.63 (t, $^3J_{H,H}$ = 7.6 Hz, 8H, *Ar*), 6.86 (t, $^3J_{H,H}$ = 7.6 Hz, 8H, *Ar*), 7.01 (d, $^3J_{H,H}$ = 7.8 Hz, 8H, *Ar*), 7.07 (d, $^3J_{H,H}$ = 7.4 Hz, 8H, *Ar*), 7.23-7.27 (m, 16H, *Ar*), 7.34 (br. s, 16H, *Ar*) ppm. ^{13}C{^{1}H} NMR (C_6D_6, 75 MHz, 25 °C): δ = 20.5 (CH_3), 20.9 (CH_3), 21.0 (CH_3), 21.2(CH_3), 120.0 (*Ar*), 120.8 (*Ar*), 120.9 (*Ar*),121.7 (*Ar*), 122.0 (*Ar*),122.6 (*Ar*), 123.4 (*Ar*), 124.9 (*Ar*), 125.2 (*Ar*), 125.5 (*Ar*), 125.7 (*Ar*), 126.0 (*Ar*), 126.9 (*Ar*), 127.7 (*Ar*), 127.2 (*Ar*), 128.6 (*Ar*), 128.9 (*Ar*), 129.2 (*Ar*), 129.6 (*Ar*), 129.3 (*Ar*), 129.8 (*Ar*), 130.1 (*Ar*), 130.6 (*Ar*), 137.9 (*Ar*), 145.3 (*Ar*), 147.0 (*Ar*), 147.3 (*Ar*), 147.4 (*Ar*), 153.2 (*Ar*), 153.5 (*Ar*), 166.2 ($ArCN_2$), 168.2 ($ArCN_2$) ppm (some signals are overlapped by C_6D_6 signals). IR (ATR) ($\tilde{\nu}$/cm^{-1}): 3436 (w), 3055 (w), 3026 (w), 2966 (m), 2863 (m), 2362 (s), 2337 (s), 1635 (s), 1588 (s), 1522 (m), 1486 (s), 1438 (s), 1424 (vs), 1386 (m), 1362 (m), 1326 (m), 1294 (m), 1220 (s), 1172 (m), 1137 (m), 1115 (m), 1068 (m), 1027 (w) 997 (w), 976 (w), 917 (m), 883 (w), 818 (w), 799 (w), 748 (vs), 695 (vs), 668 (m), 505 (s). Elemental analysis calcd (%) for $[C_{184}H_{168}Cl_4La_4N_{16}O_8]$ (3428.89): C 64.45, H 4.94, N 6.54; found C 63.59, H 5.174, N 6.02%.

Synthesis of $[\mathrm{La_2}(^{p\text{-Tolyl}}\mathrm{L_{DBF}})_2\{\mathrm{N(SiMe_3)_2}\}_2]$ (**2**)

A mixture of $^{\mathrm{p\text{-}Tolyl}}\mathrm{L_{DBF}H_2}$ (306 mg, 0.50 mmol) and $[\mathrm{La\{N(SiMe_3)_2\}_3}]$ (620 mg, 1.00 mmol) were dissolved in 15 mL of toluene and heated for 96 h at 110 °C. The cloudy mixture was filtered. The final product was recrystallized from hot toluene. The product **2** was obtained in the form of yellow crystals. ^{1}H NMR (d_8-toluene, 300 MHz, 60 °C): δ = 0.25 (s, 36H, Si*Me₃*), 0.46 (s, 3H, CH_3), 0.51 (s, 3H, CH_3), 0.70 (s, 18H, CH_3), 1.16 (thf), 3.74 (thf), 6.57 (d, $^3J_{\mathrm{H,H}}$ = 8.1 Hz, 12H, *Ar*), 6.73 (t, $^3J_{\mathrm{H,H}}$ = 7.6 Hz, 8H, *Ar*), 6.85 (d, $^3J_{\mathrm{H,H}}$ = 8.3 Hz, 12H, *Ar*), 7.05 (br. s, 2H, *Ar*), 7.12 (dd, $^3J_{\mathrm{H,H}}$ = 7.7 Hz, $^4J_{\mathrm{H,H}}$ = 1.3 Hz, 4H, *Ar*), 7.21 (dd, $^3J_{\mathrm{H,H}}$ = 7.7 Hz, $^4J_{\mathrm{H,H}}$ = 1.3 Hz, 3H, *Ar*), 7.29 (dd, $^3J_{\mathrm{H,H}}$ = 7.5 Hz, $^4J_{\mathrm{H,H}}$ = 1.3 Hz, 3H, *Ar*) ppm. ^{13}C{^{1}H} NMR (d_8-toluene, 75 MHz, 60 °C): δ = 3.7 (SiMe_3), 5.1 (CH$_3$), 25.1 (*thf*), 70.3 (*thf*), 120.1 (*Ar*), 121.0 (*Ar*), 122.5 (*Ar*), 124.4 (*Ar*), 129.6 (*Ar*), 130.3 (*Ar*),146.5 (*Ar*), 153.8 (*Ar*), 169.1 (ArCN$_2$) ppm (two of the expected aromatic carbons are overlapped by toluene-d$_8$ signals, also some signals from the free ligand are seen in ^{1}H spectrum; by recrystallization from thf solvent signals are observed). IR (ATR) ($\tilde{\nu}$/cm^{-1}): 3394 (w), 3024 (w), 2918 (m), 2852 (m), 1629 (s), 1596 (vs), 1507 (vs), 1423 (m), 1369 (m), 1330 (m), 1256 (m), 1220 (s), 1188 (m), 1145 (w), 1106 (m), 1050 (m), 937 (w), 887 (w), 811 (vs), 757 (s), 573 (m), 517 (m). Due to impurities in the bulk phase, compound **2** was not obtained as analytically pure material.

Synthesis of $[\mathrm{Sm_2}(^{p\text{-Tolyl}}\mathrm{L_{DBF}})_2\{\mathrm{N(SiMe_3)_2}\}_2(\mathrm{THF})_2]$ (**3**)

Toluene (20 ml) was condensed onto a mixture of $[\mathrm{Sm\{N(SiMe_3)_2\}_3}]$ (600 mg, 0.95 mmol) and $^{p\text{-Tol}}\mathrm{L_{DBF}H_2}$ (291 mg, 0.48 mmol). Then, the mixture was heated for 18 h at 110 °C. The yellow suspension was dried under vacuum and the yellow precipitate was washed with *n*-pentane to remove residual $[\mathrm{Sm\{N(SiMe_3)_2\}_3}]$. The remaining residue was recrystallized from hot thf to obtain bright yellow single crystals suitable for X-ray crystallography. Yield (based of single crystals): 355 mg (38 %). ^{1}H NMR (C_6D_6, 300 MHz, 25 °C): δ = -0.82 (s, 36H, SiMe_3), 0.94 (thf), 1.88 (s, 24H, CH_3), 3.40 (thf), 6.58 (t, $^3J_{\mathrm{H,H}}$ = 7.5 Hz, 4H, *Ar*), 6.74 (br. s, 16H, *Ar*), 6.96 (d, $^3J_{\mathrm{H,H}}$ = 7.0 Hz, 4H, *Ar*), 7.08 (d, $^3J_{\mathrm{H,H}}$ = 7.7 Hz, 4H, *Ar*), 7.92 (d, $^3J_{\mathrm{H,H}}$ = 6.7 Hz, 16H, *Ar*) ppm. ^{13}C{^{1}H} NMR (C_6D_6, 75 MHz, 25 °C): δ = 3.9 (SiMe_3), 21.0 (CH$_3$), 24.7 (*thf*), 69.7(*thf*), 121.4 (*Ar*), 121.0 (*Ar*), 122.7 (*Ar*), 124.7 (*Ar*), 124.7 (*Ar*), 128.1 (*Ar*), 129.5 (*Ar*), 130.1 (*Ar*),146.5 (*Ar*), 154.6 (*Ar*), 182.3 (ArCN$_2$). IR (ATR) ($\tilde{\nu}$/cm^{-1}): 3649 (w), 3441 (w), 3021 (w), 2952 (w), 2919 (w), 2919 (w), 2862 (w), 1889 (w), 1635 (m), 1596 (s), 1504 (vs), 1466 (s), 1424 (s), 1404 (m), 1322 (m), 1249 (m), 1218 (m), 1181 (s), 1148 (w), 1107 (w), 1090 (w), 1037 (w), 930 (s), 886 (m), 813 (vs), 791 (s), 756 (s), 706 (w), 617 (w), 557 (w), 490 (m). Elemental analysis calcd (%) for $[\mathrm{C_{104}H_{120}N_{10}O_4Si_4Sm_2}]$ (1987.23): C 62.86, H 6.09, 7.05; found C 62.18, H 6.15, N 6.73.

Synthesis of $^{\boldsymbol{i}\mathbf{Pr}}\mathbf{L_{Phen}H_2}$

To a solution of phenanthrene (4.0 g, 22.4 mmol) and TMEDA (7.9 ml, 52.7 mmol) in 100 mL *n*-heptane, *n*-BuLi (2.5 M in *n*-hexane, 21 ml, 52.7 mmol) was added. The mixture was heated at 70 °C for 4 hours. Upon heating, gas evolution was observed. The final dark red suspension was cooled to room temperature, and diisopropylcarbodiimide (8.69 mL, 56.1 mmol) was added to the mixture to form a light brown suspension. After stirring overnight, H_2O (150 mL) was added to the mixture. The organic phase was separated, dried under vacuum and recrystallized from hot toluene. Yield: 2.91 g (30%). ^{1}H NMR (d_8-THF, 300 MHz, 25 °C): δ = 0.11 (d, $^3J_{H,H}$ = 6.0 Hz, 6H, CH_3), 0.25 (d, $^3J_{H,H}$ =6.1 Hz, 6H, CH_3), 1.25 (d, $^3J_{H,H}$ = 5.8 Hz, 6H, CH_3), 1.32 (d, $^3J_{H,H}$ =6.6 Hz, 6H, CH_3), 1.46-2.02 (m, 2H, *CH*), 4.06-4.14 (m, 2H, *CH*), 4.63 (s, 2H, *NH*), 7.57 (t, $^3J_{H,H}$ = 7.5 Hz, 2H, *Ar*), 7.64 (dd, $^3J_{H,H}$ = 7.3 Hz, $^4J_{H,H}$ = 1.7 Hz, 2H, *Ar*), 7.68 (s, 2H, *Ar*), 7.86 (dd, $^3J_{H,H}$ = 7.6 Hz, $^4J_{H,H}$ = 1.7 Hz, 2H, *Ar*) ppm. ^{13}C{^{1}H} NMR (d_8-THF, 75 MHz, 25 °C): δ = 22.5 (CH_3), 23.2 (CH_3), 23.5 (CH_3), 43.9 (*C*H), 50.4 (*C*H), 127.7 (*Ar*), 128.4 (*Ar*), 129.4(*Ar*), 130.2 (*Ar*), 130.8 (*Ar*), 134.3 (*Ar*), 135.9 (*Ar*),156.3 (Ar*C*N_2) (One of the signals of one CH_3 carbon atom overlapps with signals of THF. This signals has been detected in a ^{1}H/^{13}C-HMQC NMR spectrum in C_6D_6 (Fig. S24)). IR (ATR) ($\tilde{\nu}$/cm^{-1}): 3421 (w), 3364 (w), 3045 (w), 2958 (w), 2923 (w), 2864 (w), 1617 (vs), 1563 (w), 1521 (w), 1469 (s), 1434 (m), 1379 (m), 1356 (m), 1342 (m), 1317 (m), 1279 (w), 1256 (s), 1200 (w), 1174 (s), 1132 (m), 1114 (m), 1033 (w), 986 (w), 941 (w), 924 (w), 890 (w), 861 (w), 843 (s), 830 (s), 820 (m), 784 (w), 765 (w), 732 (s), 659 (w), 647 (w), 604 (w), 566 (w), 516 (w), 478 (w), 466 (w), 421 (w). Elemental analysis calcd (%) for [$C_{28}H_{38}N_4$] (430.31): C 78.09, H 8.89, N 13.01; found C 77.93, H 8.84, N 12.77.

Synthesis of [Sm{$^{iPr}L_{Phen}$}(N(SiMe$_3$)$_2$)(thf)] (**4**)

A mixture of [Sm{N(SiMe$_3$)$_2$}$_3$] (700 mg, 1.11 mmol) and $^{iPr}L_{Phen}H_2$ (434 mg, 1.00 mmol) was dissolved in THF (20 ml) and stirred for 3 d at 65 °C. After the solvent was removed under vacuum, the yellow precipitate was washed with *n*-pentane and recrystallized from hot THF. Yellow single crystals were obtained after 5 h at room temperature. Yield: 477 mg (58%). ^{1}H NMR (d_8-THF, 300 MHz, 25 °C): δ = -5.75 (s, 3H, CHC*H*$_3$), -1.61 (d, $^3J_{H,H}$ =6.0 Hz, 3H, CHC*H*$_3$), -1.15 (s, 3H, CHC*H*$_3$), -0.72 ((d, $^3J_{H,H}$ = 5.5 Hz, 3H, CHC*H*$_3$), -1.05 – -0.01 (br. s, 18H, SiC*H*$_3$), -0.15 – -0.02 (m, 2H, C*H*(CH$_3$)$_2$), 0.19 (d, $^3J_{H,H}$ = 6.1 Hz, 3H, CHC*H*$_3$), 0.96 (d, $^3J_{H,H}$ = 6.0 Hz, 3H, CHC*H*$_3$), 1.88 (d, $^3J_{H,H}$ =6.0 Hz, 3H, CHC*H*$_3$), 3.96-4.04 (m, 1H, C*H*(CH$_3$)$_2$), 4.60 (s, 3H, CHC*H*$_3$), 5.11 (s, 1H, *Ar*), 6.67 (t, $^3J_{H,H}$ = 7.4 Hz, 1H, *Ar*), 6.82-6.90 (m, 1H, C*H*(CH$_3$)$_2$), 7.32 (d, $^3J_{H,H}$ = 7.2 Hz, 1H, *Ar*), 7.63 (d, $^3J_{H,H}$ = 8.0 Hz, 1H, *Ar*), 7.80 (t, $^3J_{H,H}$ = 7.5 Hz, 1H, *Ar*), 7.90 (d, $^3J_{H,H}$ = 8.7 Hz, 1H, *Ar*), 8.10 (d, $^3J_{H,H}$ = 8.7 Hz, 1H, *Ar*), 8.35 (d, $^3J_{H,H}$ = 7.9 Hz, 1H, *Ar*) ppm. ^{13}C{^{1}H} NMR (d_8-THF, 75 MHz, 25 °C): δ = 5.7(Si(*C*H$_3$)$_3$), 14.3 (*C*H$_3$), 18.0 (*C*H$_3$), 22.0 (*C*H$_3$), 22.1 (*C*H$_3$), 24.8 (*C*H$_3$), 24.8 (*C*H$_3$), 26.5 (*C*H$_3$), 27.6 (*C*H$_3$), 46.7(*C*H(CH$_3$)$_3$), 51.1 (*C*H(CH$_3$)$_3$), 52.6 (*C*H(CH$_3$)$_3$), 53.9 (*C*H(CH$_3$)$_3$), 126.8 (*Ar*), 127.0 (*Ar*), 127.3 (*Ar*), 128.4 (*Ar*), 128.6 (*Ar*), 129.3 (*Ar*), 130.4 (*Ar*), 131.5 (*Ar*), 132.6 (*Ar*), 133.9 (*Ar*), 134.1 (*Ar*), 134.5 (*Ar*), 136.6 (*Ar*), 144.3 (*Ar*), 177.4 (ArCN$_2$) ppm (some small peaks from the free ligand are observed in the NMR spectrum). IR (ATR) ($\tilde{\nu}$/cm^{-1}): 3423 (w), 3362 (w), 3088 (w), 3047 (w), 2960 (vs), 2652 (w), 2607 (w), 1619 (s), 1553 (m), 1522 (m), 1465 (s), 1436 (m), 1376 (m), 1356 (m), 1338 (m), 1315 (m), 1251 (s), 1175 (m), 1132 (m), 1114 (m), 1069 (w), 1039 (w), 1016 (w), 990 (s), 921 (w), 869 (m), 827 (s), 733 (m), 666 (w), 635 (78), 605 (w), 542 (w), 521 (w), 474 (w) cm^{-1}. Elemental analysis calcd (%) for [$C_{38}H_{62}N_5OSi_2Sm$] (811.48): C 56.25, H 7.70, N 8.63; found C 56.64, H 7.57, N 8.93.

X-ray Crystallographic Studies

A suitable crystal was covered in mineral oil (Aldrich) and mounted on a glass fiber. The crystal was transferred directly to the cold stream of a STOE IPDS 2 or STOE StadiVari diffractometer.

All structures were solved by using the program SHELXS/T.[2] The remaining non-hydrogen atoms were located from successive difference Fourier map calculations. The refinements were carried out by using full-matrix least-squares techniques on F^2, by minimizing the function $(F_o\text{-}F_c)^2$, where the weight was defined as $4F_0^2/2(F_o^2)$ and F_o and F_c were the observed and calculated structure factor amplitudes, respectively, by using the program SHELXL.[2] The hydrogen atom contributions of all of the compounds were calculated, but not refined. In each case, the locations of the largest peaks in the final difference Fourier map calculations, as well as the magnitude of the residual electron densities, were of no chemical significance. Positional parameters, hydrogen atom parameters, thermal parameters, bond distances and angles have been deposited as supporting information. CCDC 1515852, 1515853, 1515855-1515857, 1520430, and 1515853.

Table S 1. Crystal data and structure refinement for $^{p\text{-Tolyl}}\mathbf{L}_{\mathbf{DBF}}\mathbf{H}_2$ and $^{i\text{Pr}}\mathbf{L}_{\mathbf{Phen}}\mathbf{H}_2$.

Compound reference	$^{\text{p-Tolyl}}\mathbf{L}_{\mathbf{DBF}}\mathbf{H}_2$	$^{i\text{Pr}}\mathbf{L}_{\mathbf{Phen}}\mathbf{H}_2$
Chemical formula	$C_{42}H_{36}N_4O \cdot 2(C_2H_6OS)$	$C_{28}H_{38}N_4$
Formula Mass	769.00	430.62
Crystal system	Triclinic	monoclinic
***a*/Å**	9.7749(4)	17.381(3)
***b*/Å**	10.2099(4)	8.9219(8)
***c*/Å**	21.6219(10)	18.170(3)
α**/°**	78.582(4)	90
β**/°**	80.858(4)	114.373(11)
γ**/°**	89.827(4)	90
Unit cell Volume/Å^3	2087.41(16)	2566.5(6)
Temperature/K	200	150.0
Space group	$P\bar{1}$	$P2_1/n$
No. of formula units per unit cell, Z	2	4
Radiation type	MoKα	MoKα
Absorption coefficient, *m*/mm^{-1}	0.172	0.066
No. of reflections measured	18610	16536
No. of independent reflections	9492	5042
R_{int}	0.0613	0.0779
Final R_1 values ($I>2\sigma(I)$)	0.0594	0.0566
Final $wR(F^2)$ values ($I>2\sigma(I)$)	0.1686	0.1343
Final R_1 values (all data)	0.0747	0.0898
Final $wR(F^2)$ values (all data)	0.1809	0.1476
Goodness of fit on F^2	1.050	0.906

Table S 2. Crystal data and structure refinement for complexes **1-4**.

Compound reference	**1**[*]	**2**[+]	**3**	**4**
Chemical formula	$C_{184}H_{168}Cl_4La_4N_{16}O_8$	$2(C_{96}H_{104}La_2N_{10}O_2Si_4) \cdot 9(C_7H_8)$	$C_{104}H_{120}N_{10}O_4Si_4Sm_2 \cdot 3(C_4H_8O)$	$C_{104}H_{120}N_{10}O_4Si_4Sm_2 \cdot 3(C_4H_8O)$
Formula Mass	3428.77	4467.32	2203.46	811.45
Crystal system	triclinic	monoclinic	triclinic	monoclinic
***a*/Å**	21.2533(4)	20.8963(9)	16.7981(17)	13.2427(3)
***b*/Å**	21.6170(4)	22.8615(8)	18.7804(19)	19.5465(3)
***c*/Å**	25.3669(5)	25.1772(10)	19.323(2)	16.2000(3)
α/°	75.2440(10)	90	82.107(9)	90
β/°	83.199(2)	94.338(3)	81.378(9)	106.627(2)
γ/°	82.524(2)	90	68.045(8)	90
Unit cell Volume/Å^3	11129.9(4)	11993.2(8)	5567.9(11)	4018.01(14)
Temperature/K	200.0	150(2)	150.0	100.0
Space group	$P\bar{1}$	$P2/n$	$P\bar{1}$	$P2_1/n$
No. of formula units per unit cell, Z	2	4	2	4
Radiation type	MoKα	MoKα	MoKα	MoKα
Absorption coefficient, *m*/mm^{-1}	0.846	0.781	1.145	1.556
No. of reflections measured	188811	76389	37109	51628
No. of independent reflections	188811	23699	21650	7917
R_{int}	0.0860	0.1342	0.0661	0.0247
Final R_1 values ($I>2\sigma(I)$)	0.0867	0.1308	0.0558	0.0169
Final $wR(F^2)$ values ($I>2\sigma(I)$)	0.2232	0.2810	0.1305	0.0399
Final R_1 values (all data)	0.1467	0.2382	0.1025	0.0197
Final $wR(F^2)$ values (all data)	0.2751	0.3663	0.1429	0.0407
Goodness of fit on F^2	1.027	1.103	0.841	1.040

[*] The crystals of **1** are systematically twined. The reflections of twin domains are in close proximity. Upon integration of the data set using the programs STOE X-RED,[3] X-SHAPE,[4] and LANA (part of X-Area 1.75)[5] part of the information got lost. This results in incomplete data sets. The structure than refined as a 2-component perfect twin.

The structure was refined with nine molecules of strongly disordered toluene solvent molecules and also by supressing these molecules using “Squeeze”.[6] Both version have been deposited as cif file (sse also Figures S2a and 2b) The data shown in the table corresponds to the version with supressed solvent molecules.

[+] As result of the large amount of solvent within the crystal we faced problems upon preparation. Even under very careful preparation, the solvent diffuses out of the crystal surface and thus alters the surface.

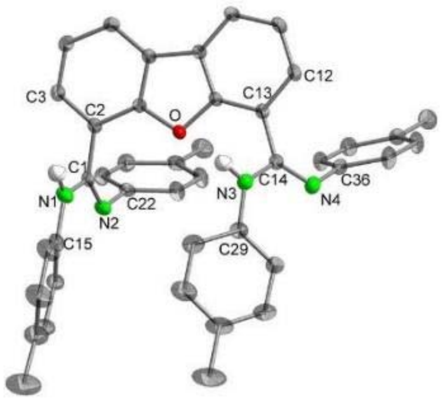

Figure S 1. Molecular structure of $^{p\text{-Tolyl}}\mathbf{L}_{\mathbf{DBF}}\mathbf{H}_2$ in the solid state (displacement ellipsoids are scaled to the 30% probability level; omitting carbon bound hydrogen atoms for clarity). Selected bond lengths [Å], angles [°]: C1-C2 1.502(2), C13-C14 1.498(2), C1-N1 1.364(2), C1-N2 1.281(2), C14-N3 1.370(2), C14-N4 1.287(2), N1-C15 1.405(2), N2-C22 1.422(2), N3-C29 1.404(2), N4-C36 1.416(2); N1-C1-N2 122.73(1), N3-C14-N4 121.79(2), C1-C2-C3 123.85(1), C12-C13-C14 122.90(2).

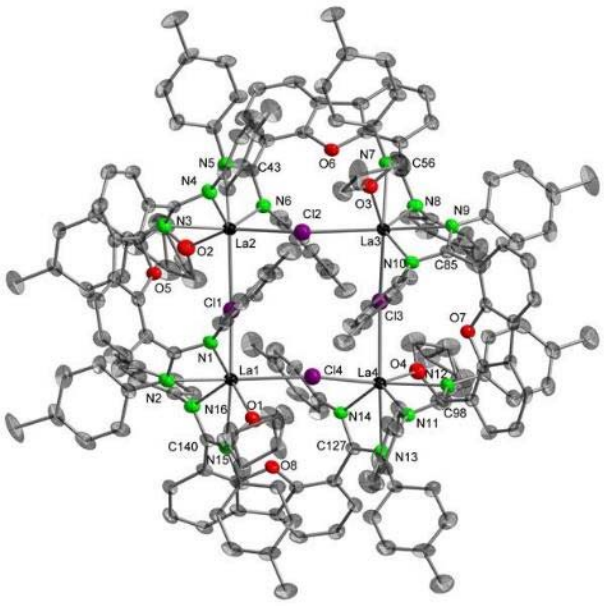

Figure S2a. Molecular structure of **1** in the solid state (displacement ellipsoids are scaled to the 30% probability level; omitting carbon bound hydrogen atoms and solvent molecules for clarity). Selected bond lengths [Å], angles [°]: La1-N1 2.531(9), La1-N2 2.546(9), La1-N15 2.505(9), La1-N16 2.556(9), La1-Cl1 2.857(3), La1-Cl4 2.885(3), La2-N3 2.504(9), La2-N4 2.547(9), La2-N5 2.547(9), La2-N6 2.539(9), La2-Cl1 2.880(3), La2-Cl2 2.863(3), La3-N7 2.483(9), La3-N8 2.549(9), La3-N9 2.561(8), La3-N10 2.529(9), La3-Cl2 2.881(3), La3-Cl3 2.881(3), La4-N11 2.556(8), La4-N12 2.481(9), La4-N13 2.563(9), La4-N14 2.512(8), La1-Cl1 2.857(3), La1-Cl4 2.885(3), La2-Cl1 2.880(3), La2-Cl2 2.863(3), La3-Cl2 2.881(3), La3-Cl3 2.881(3), La4-Cl3 2.889(3), La4-Cl4 2.852(3), La1-O1 2.543(8), La2-O2 2.546(8), La3-O3 2.548(7), La4-O4 2.581(8), La4-Cl3 2.889(3), La4-Cl4 2.852(3); N1-La1-N2 52.2(3), N15-La1-N16 53.1(3), N3-La2-N4 53.8(3), N5-La2-N6 52.1(3), N7-La3-N8 52.8(3), N9-La3-N10 52.8(3), N11-La4-N12 52.6(3), N13-La4-N14 52.2(3), La1-Cl1-La2 151.06(14), La2-Cl2-La3 148.83(12), La3-Cl3-La4 150.15(12), La4-Cl4-La1 151.17(12).

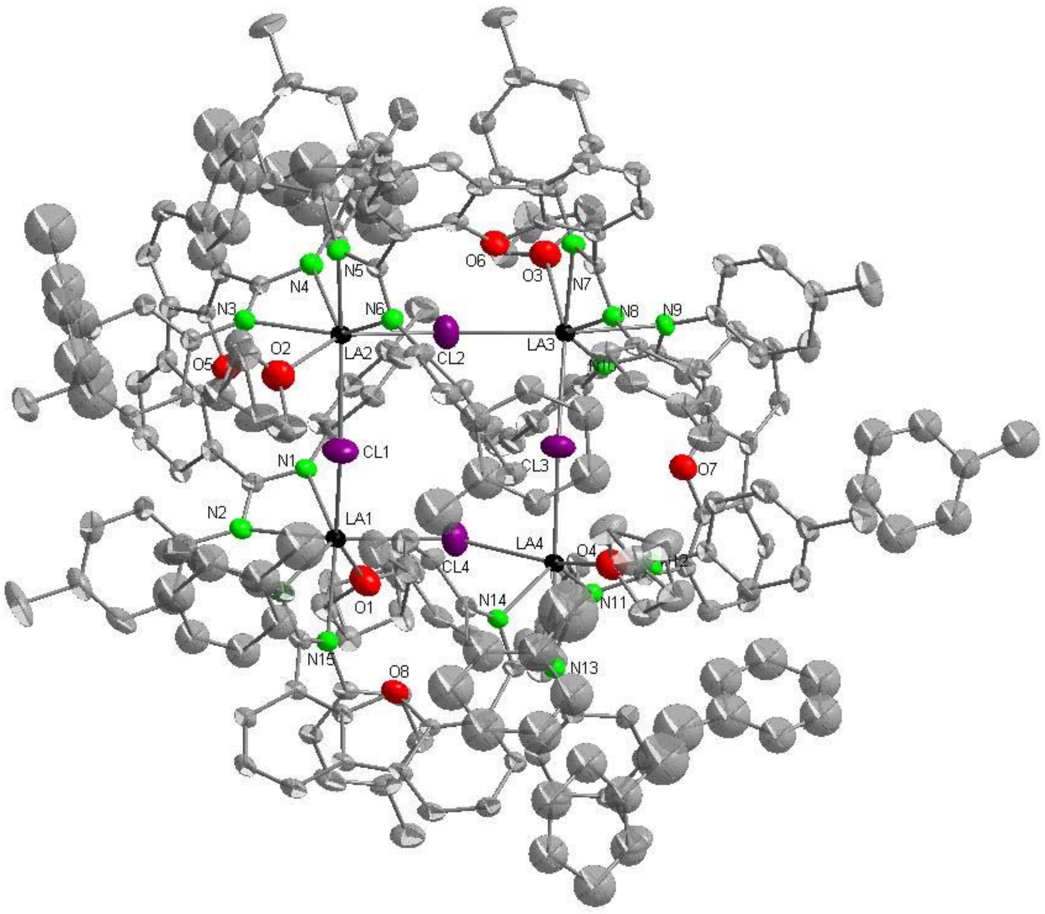

Figure S2b. Molecular structure of **1** in the solid state (displacement ellipsoids are scaled to the 30% probability level; omitting carbon bound hydrogen atoms for clarity) showing additional all toluene molecules.

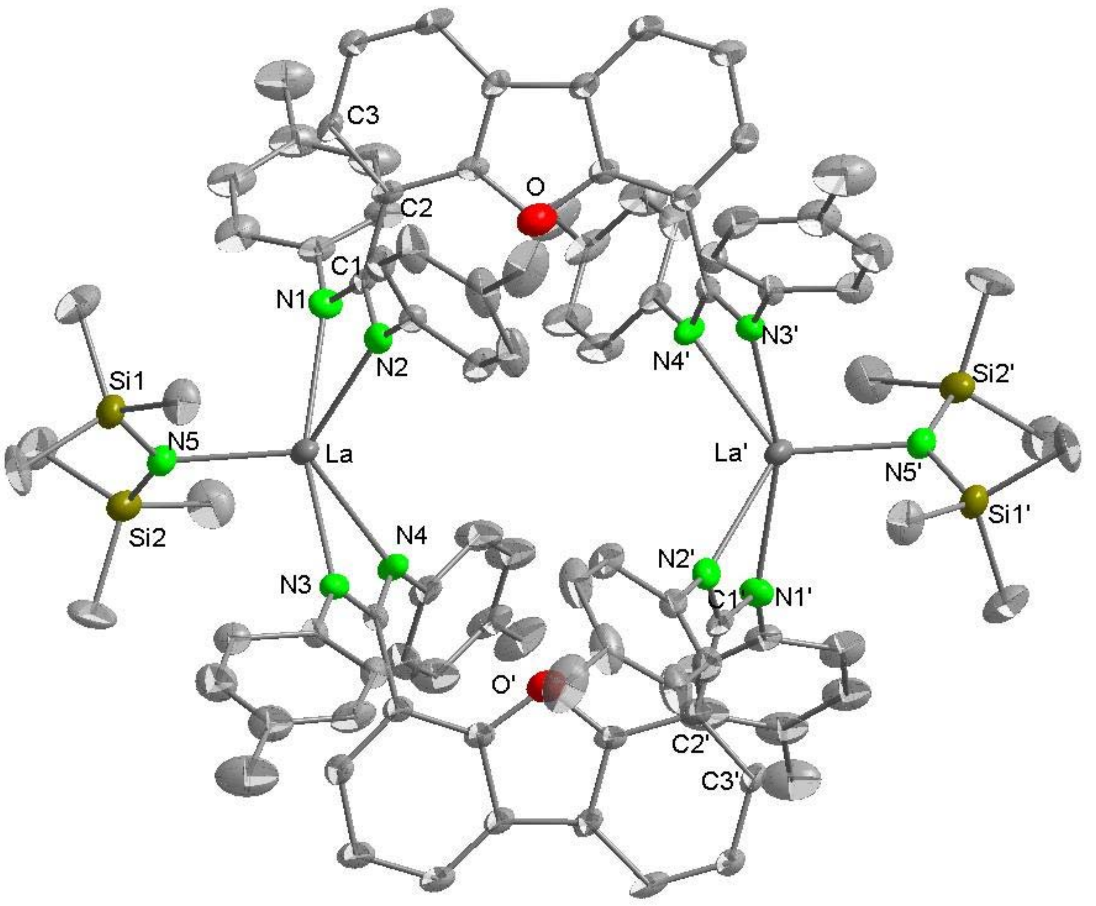

Figure S3. Molecular structure of **2** in the solid state (displacement ellipsoids are scaled to the 30% probability level; omitting carbon bound hydrogen atoms and solvent molecules for clarity). Selected bond lengths [Å], angles [°]: La-N1 2.557(11), La-N2 2.487(12), La-N3 2.528(10), La-N4 2.513(10), La-N5 2.319(10), N5-Si1 1.686(11), N5-Si2 1.710(12), C1-N1 1.33(2), C1-N2 1.33(2), N3-C14 1.33(2), N4-C14 1.32(2); N1-La-N2 53.6(4), N3-La-N4 53.5(4), N1-C1-N2 118.1(12), N3-C14-N3 117.9(11).

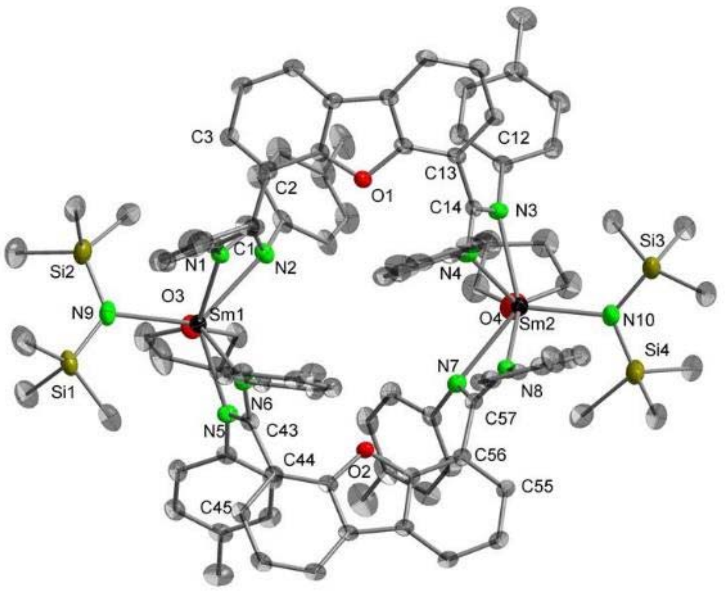

Figure S4. Molecular structure of **3** in the solid state (displacement ellipsoids are scaled to the 30% probability level; omitting carbon bound hydrogen atoms and solvent molecules for clarity). Selected bond lengths [Å], angles [°]: Sm1-N1 2.412(5), Sm1-N2 2.480(5), Sm1-N5 2.446(5), Sm1-N6 2.429(4), Sm1-N9 2.315(5), Sm1-O3 2.466(4), Sm2-N3 2.495(5), Sm2-N4 2.411(6), Sm2-N7 2.516(5), Sm2-N8 2.398(5), Sm2-N10 2.326(5), Sm2-O4 2.494(6), N9-Si1 1.701(6), N9-Si2 1.718(6), N10-Si31.702(7), N10-Si4 1.607(11), C1-N1 1.323(7), C1-N2 1.315(8), C14-N3 1.322(8), C14-N4 1.320(8), C1-C2 1.545(7), C13-C14 1.531(7), C43-C44 1.522(7), C56-C57 1.540(6); N1-Sm1-N2 53.72(2), N5-Sm1-N6 54.54(16), N3-Sm2-N4 53.93(2), N7-Sm2-N8 54.48(2), N1-C1-N2 113.9(6), C1-C2-C3 116.3(3), N3-C14-N4 114.8(6), C12-C13-C14 118.9(3), N5-C43-N6 113.9(5), C43-C44-C45 117.7(3), N7-C57-N8 114.6(5), C55-C56-C57 116.0(3), Si1-N9-Si2 122.3(3), Si3-N10-Si4 119.4(5).

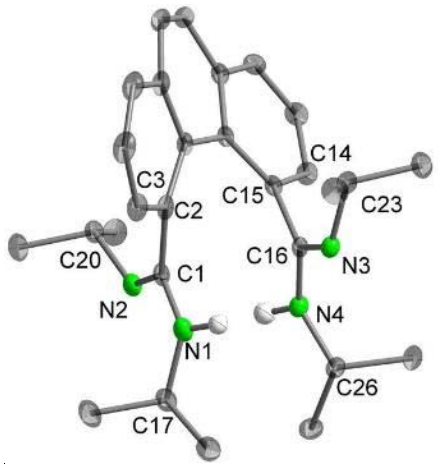

Figure S5. Molecular structure of **$^{iPr}L_{Phen}H_2$** in the solid state (displacement ellipsoids are scaled to the 30% probability level; omitting carbon bound hydrogen atoms for clarity). Selected bond lengths [Å], angles [°]: C1-N1 1.379(3), C1-N2 1.284(3), C1-C2 1.505(3), N1-C17 1.461(3), N2-C20 1.461(3), C16-N3 1.286(2), C16-N4 1.375(2), N3-C23 1.463(2), N4-C26 1.457(3); C1-C2-C3 115.55(2), C14-C15-C16 113.68(2), N1-C1-N2 119.28(2), N3-C16-N4 119.38(2).

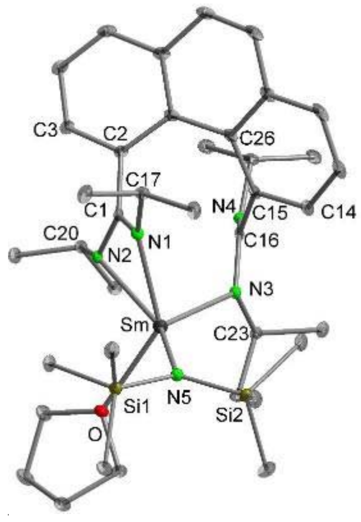

Figure S6. Molecular structure of **4** in the solid state (displacement ellipsoids are scaled to the 30% probability level; omitting carbon bound hydrogen atoms for clarity). Sm1-N1 2.3143(12), Sm1-N2 2.4666(12), Sm1-N3 2.3191(13), Sm1-N5 2.3401(13), Sm1-O1 2.5270(11), N1-C1 1.351(2), N1-C17 1.4677(19), N2-C1 1.3257(19), N2-C20 1.4735(19), N3-C16 1.386(2), N3-C23 1.4818(19), N4-C16 1.289(2), N4-C26 1.4577(19), Si1-N5 1.7115(13), Si2-N5 1.7131(13); N1-Sm1-N2 56.28(4), N1-C1-N2 115.09(1), C1-C2-C3 114.62(1), N3-C16-N4 120.92(1), C14-C15-C16 111.31(1), Si1-N5-Si2 122.25(8).

NMR Spectra of the Ligands and Metal Complexes

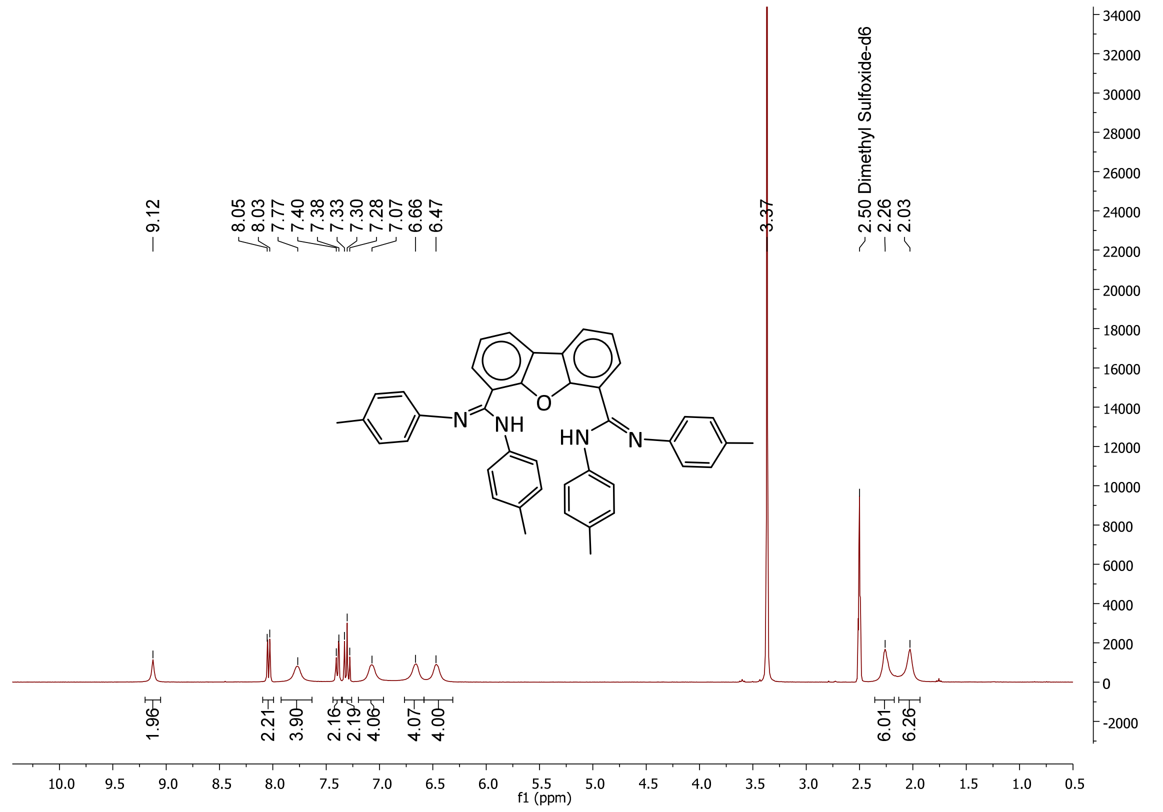

Figure S7. ^{1}H NMR spectrum of $^{p\text{-Tolyl}}\mathbf{L}_{\mathbf{DBF}}\mathbf{H}_2$ in DMSO-d_6.

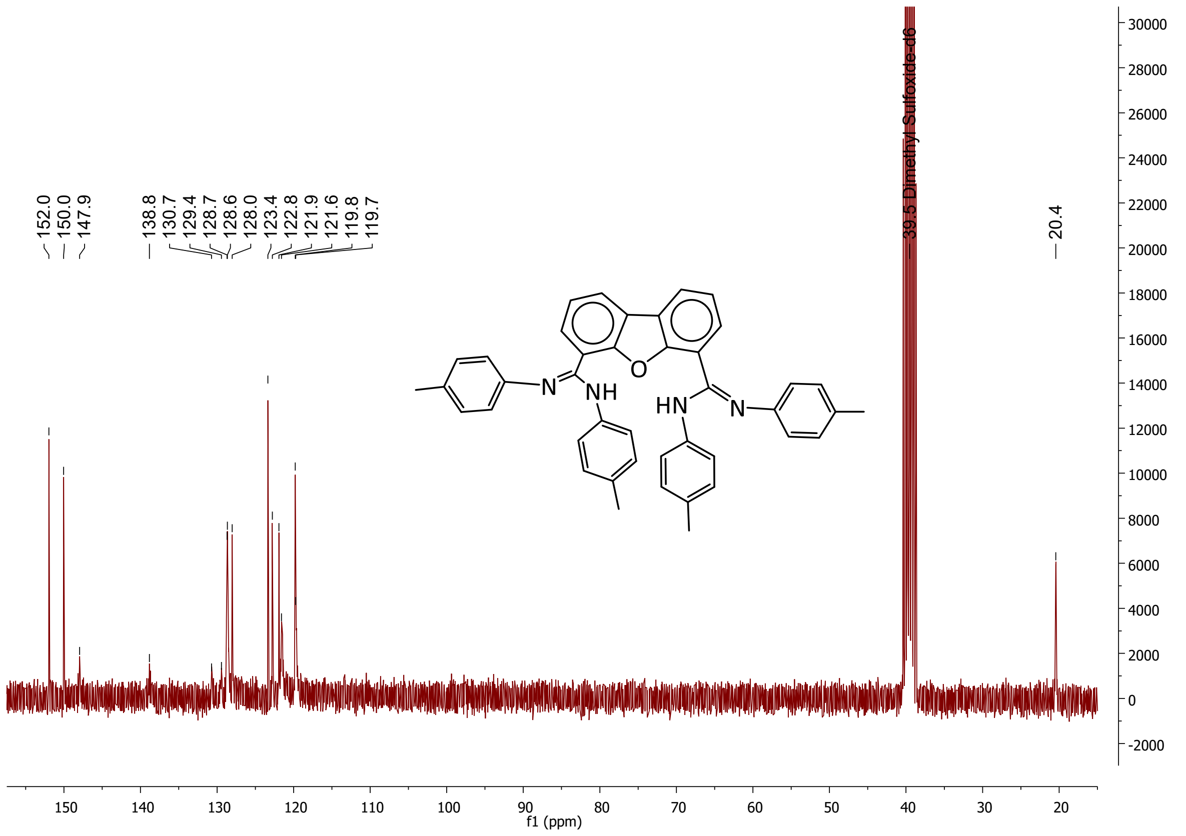

Figure S8. ^{13}C{^{1}H} NMR spectrum of $^{p\text{-Tolyl}}\mathbf{L}_{\mathbf{DBF}}\mathbf{H}_2$ in DMSO-d$_6$.

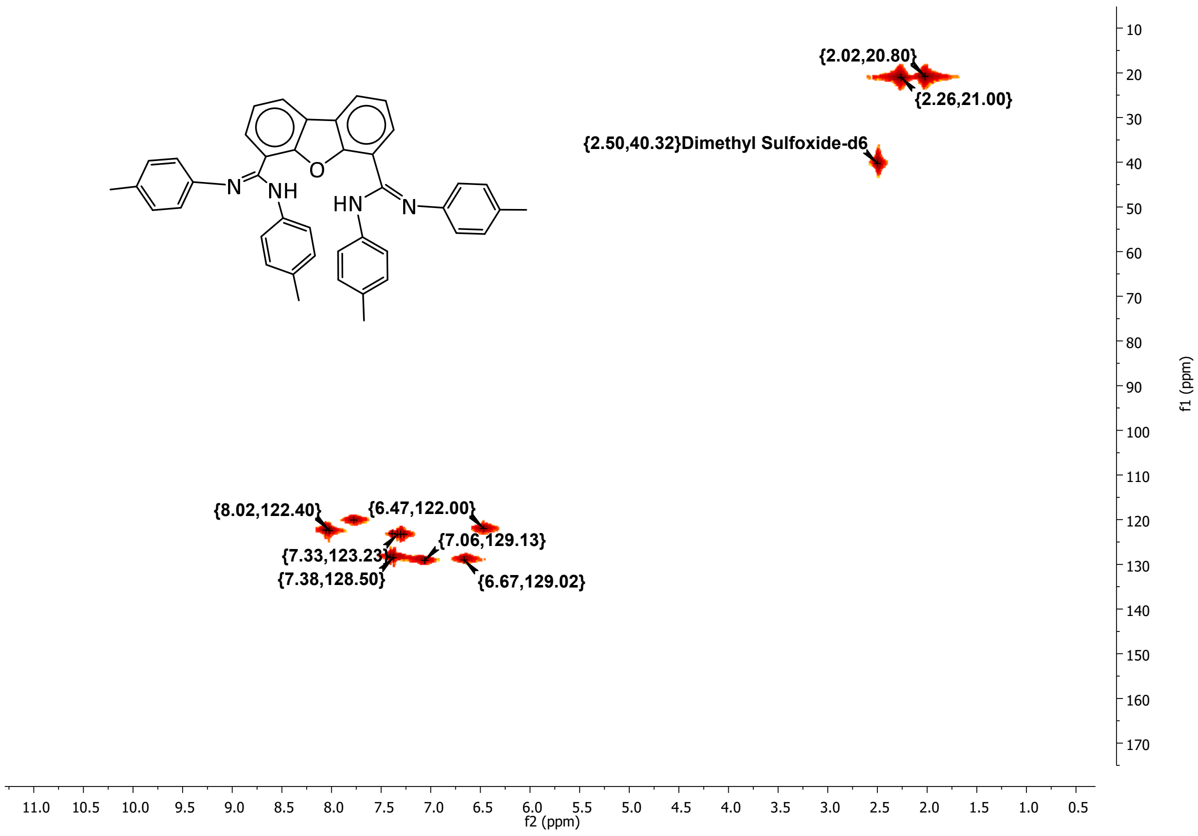

Figure S9. ^{1}H/^{13}C-HMQC NMR spectrum of $^{\text{p-Tolyl}}\mathbf{L_{DBF}H_2}$ in DMSO-d$_6$.

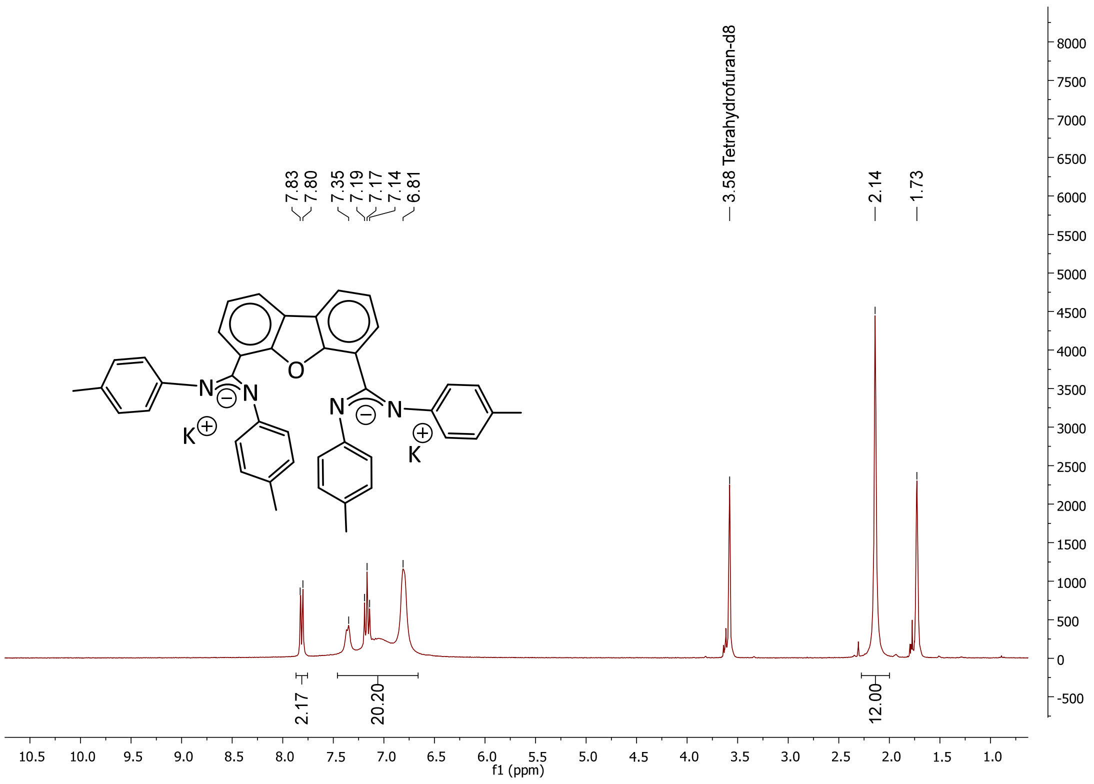

Figure S10. ^{1}H NMR spectrum of $^{\text{p-Tolyl}}\mathbf{L_{DBF}K_2}$ in THF-d$_8$.

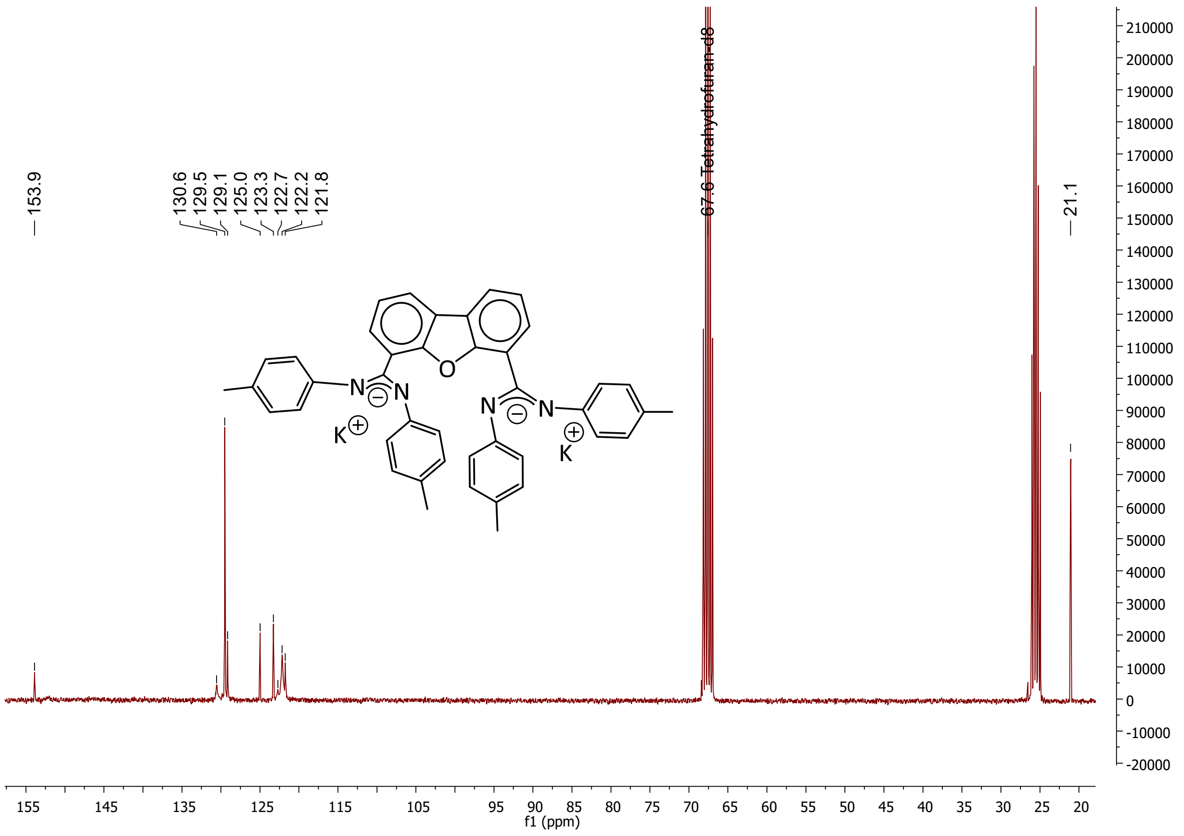

Figure S11. $^{13}C\{^{1}H\}$ NMR spectrum of $^{\mathbf{p\text{-}Tolyl}}\mathbf{L_{DBF}K_2}$ THF-d_8.

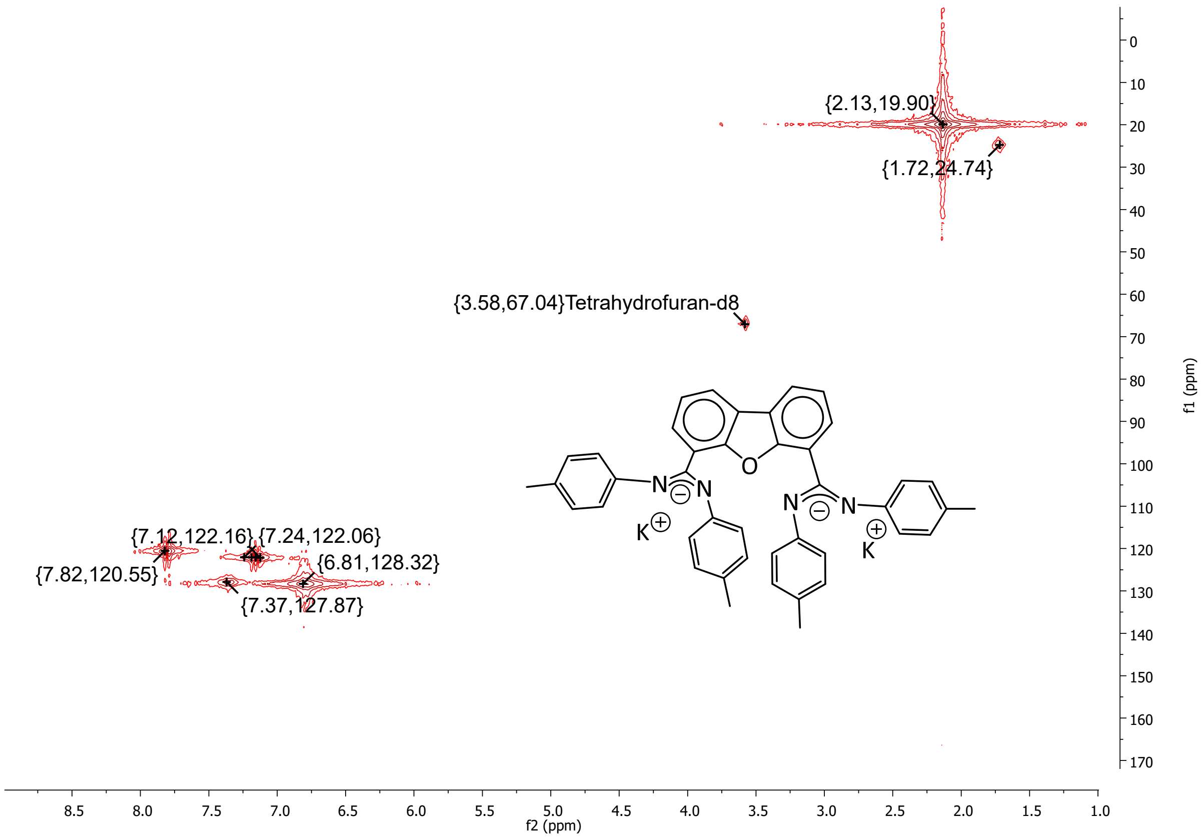

Figure S12. $^{1}H/^{13}C$-HMQC NMR spectrum of $^{\mathbf{p\text{-}Tolyl}}\mathbf{L_{DBF}K_2}$ in THF-d_8.

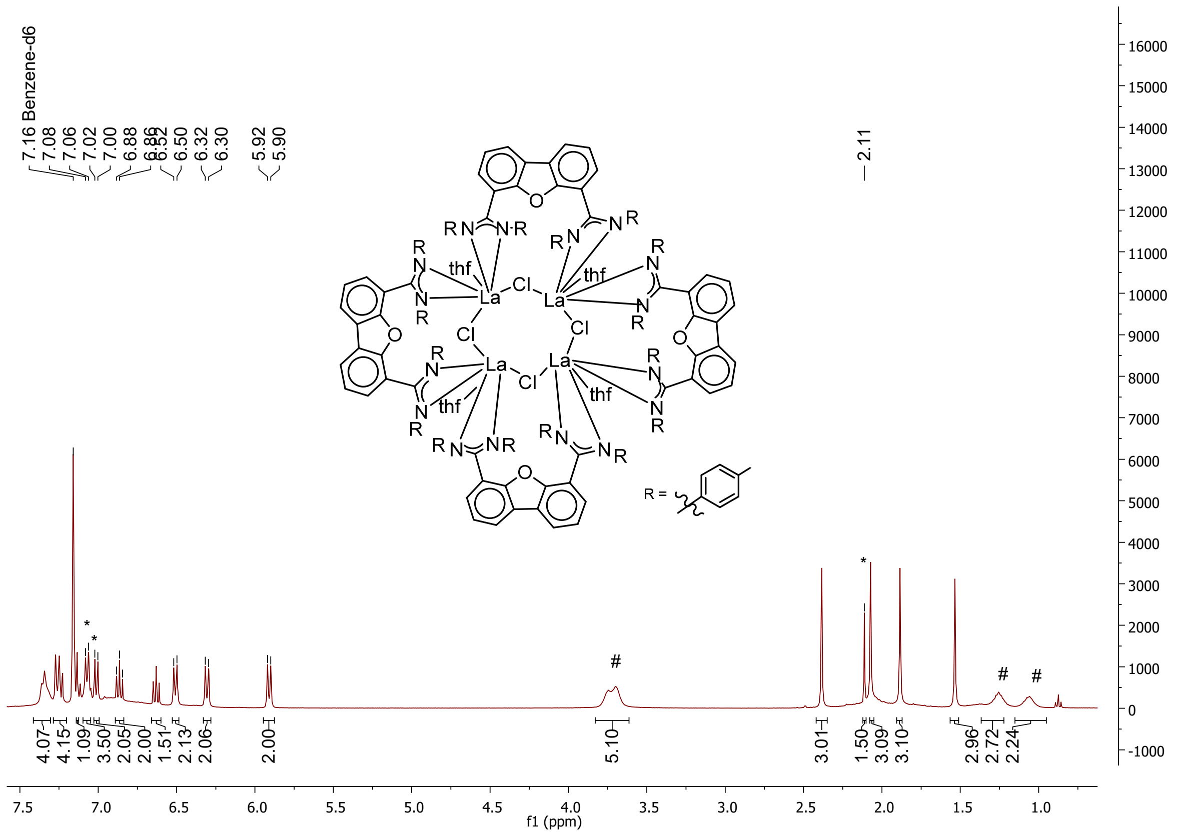

Figure S 13. ^{1}H NMR spectrum of [La$_4$(μ-Cl)$_4$($^{p\text{-Tolyl}}$L$_{DBF}$)$_4$(THF)$_4$] (**1**) at 25 °C, * toluene, $^{\#}$ coordinated THF, in C_6D_6. The numbers under the integrals are canceled down to one ligand.

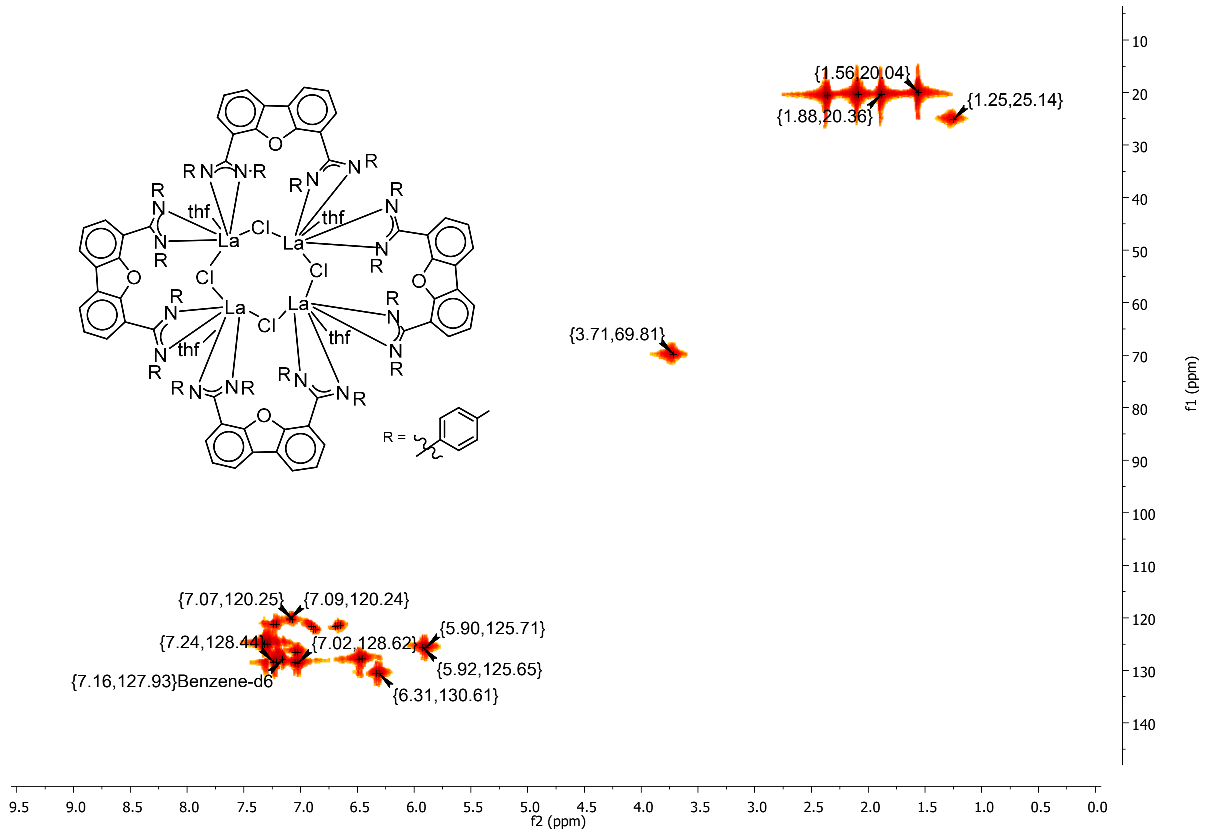

Figure S14. ^{1}H/^{13}C-HMQC NMR spectrum of [La$_4$(μ-Cl)$_4$($^{p\text{-Tolyl}}$L$_{DBF}$)$_4$(THF)$_4$] (**1**) at 60 °C in C_6D_6.

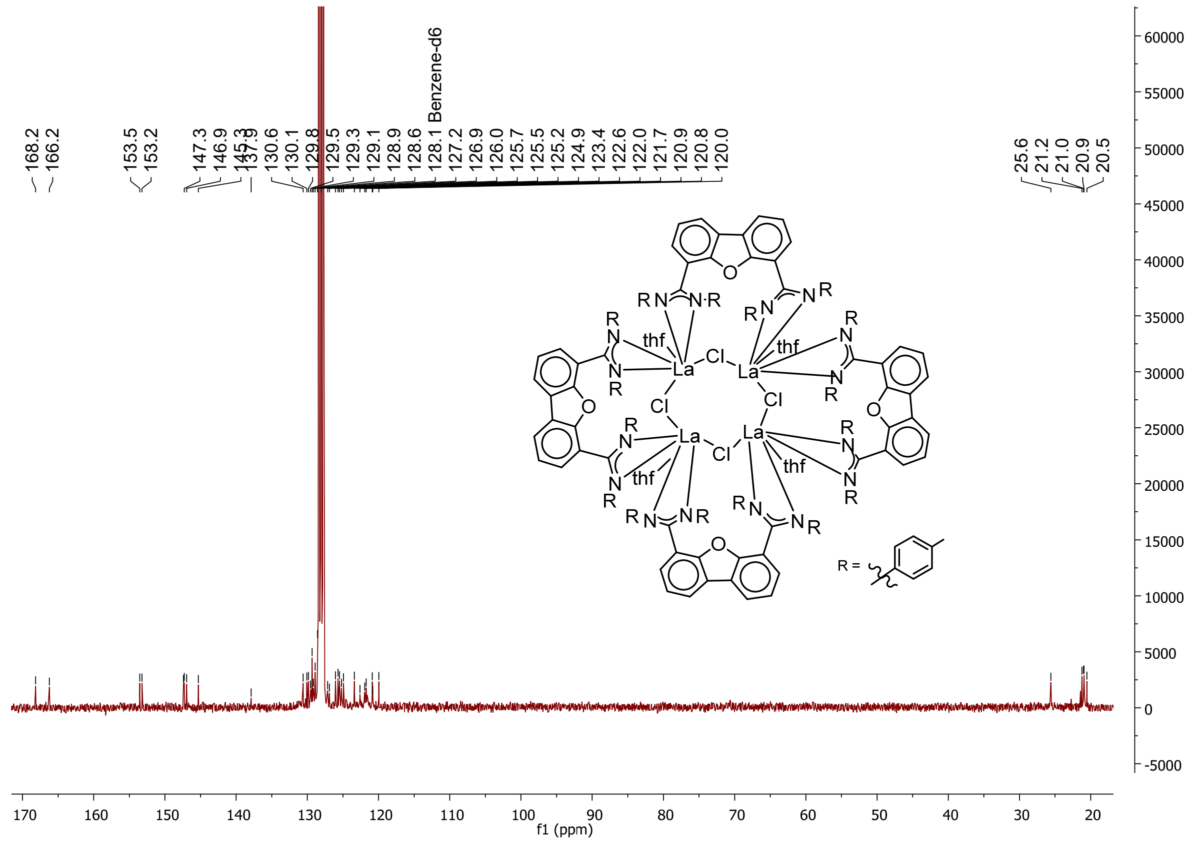

Figure S15. ^{13}C{^{1}H} NMR spectrum NMR spectrum of [La$_4$(μ-Cl)$_4$($^{p\text{-Tolyl}}$L$_{DBF}$)$_4$(THF)$_4$] (**1**) at rt in C_6D_6.

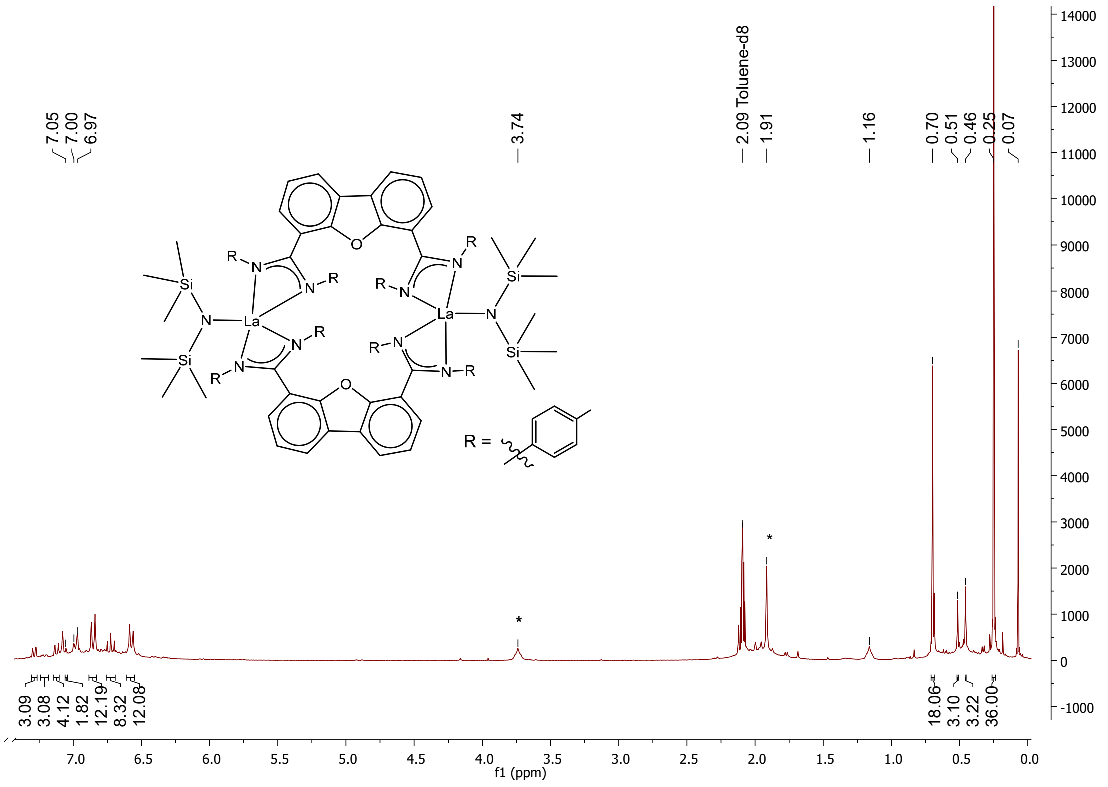

Figure S16. ^{1}H NMR spectrum of [La$_2$($^{p\text{-Tolyl}}$L$_{DBF}$)$_2${N(SiMe$_3$)$_2$}$_2$] (**2**) at 60 °C in toluene-d$_8$. * THF. Due to impurities in the bulk phase, compound **2** was not obtained as analytically pure material.

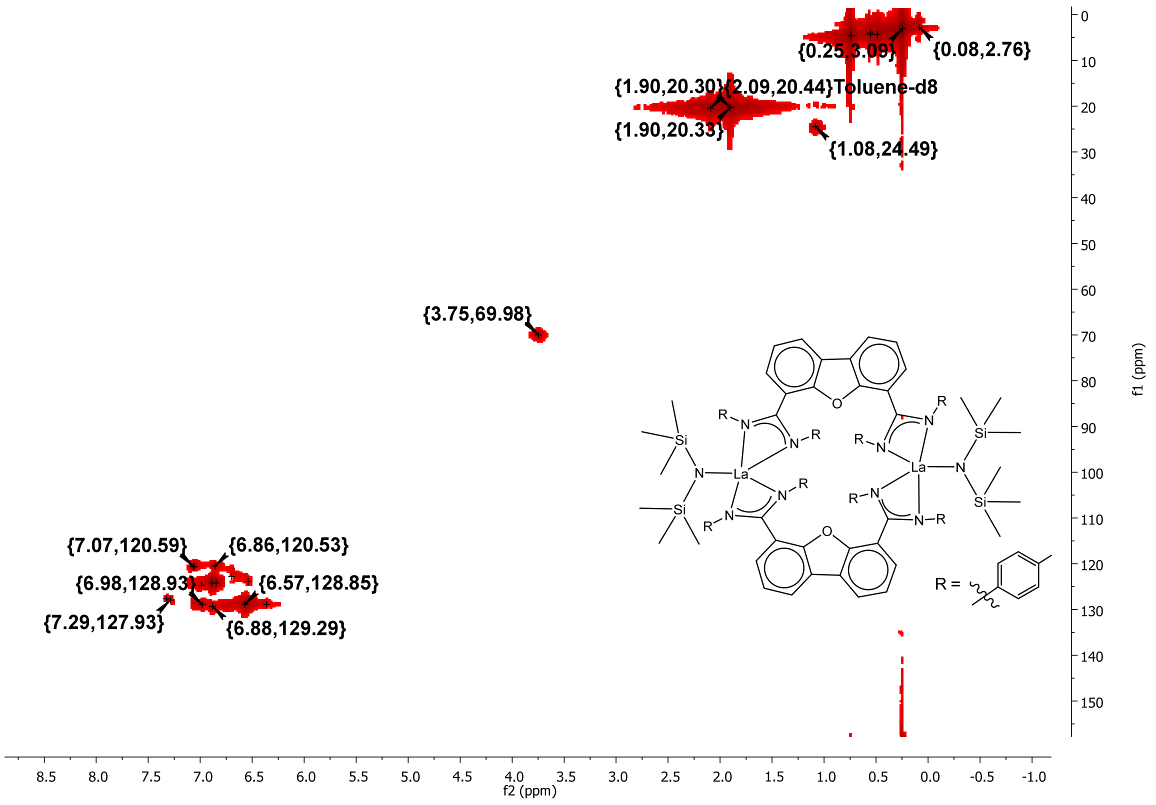

Figure S17. ^{1}H/^{13}C-HMQC NMR spectrum of [La$_2$($^{p\text{-Tolyl}}$L$_{DBF}$)$_2${N(SiMe$_3$)$_2$}$_2$] (**2**) at rt toluene-d$_8$.

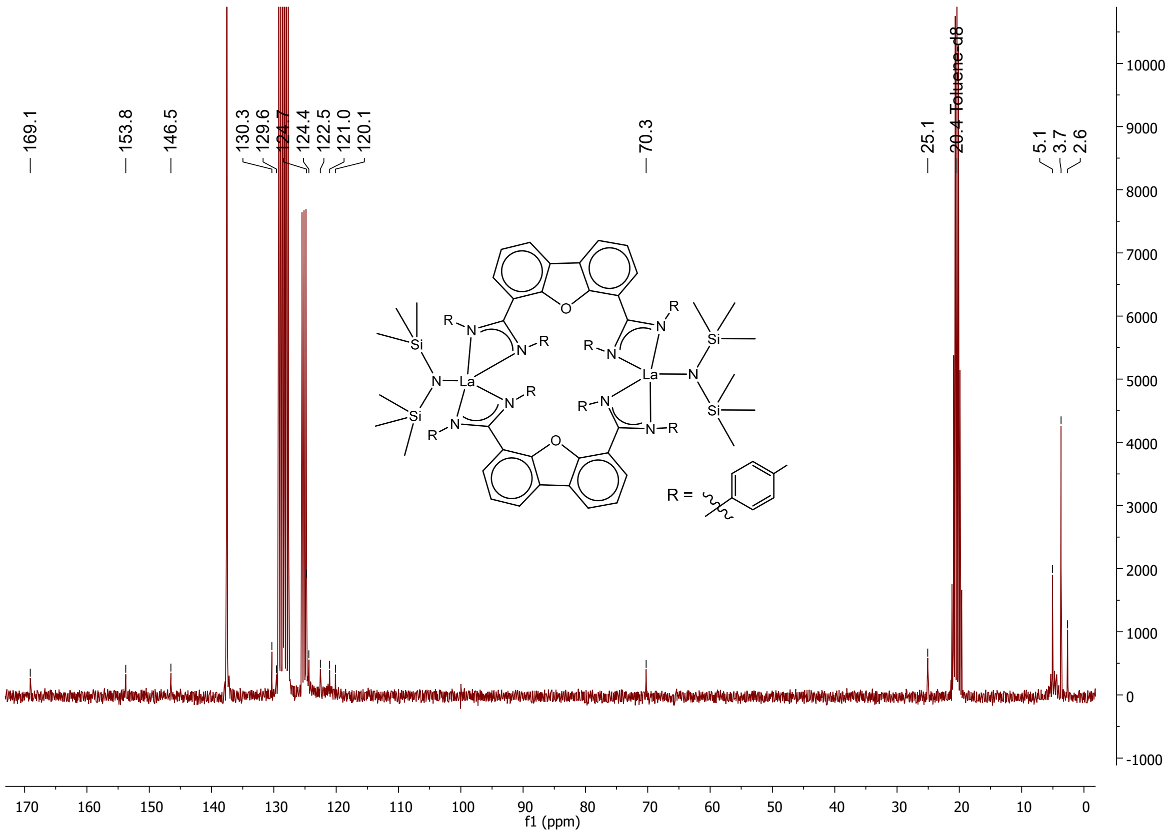

Figure S18. $^{13}C\{^{1}H\}$ NMR spectrum of $[La_2(^{p\text{-Tolyl}}L_{DBF})_2\{N(SiMe_3)_2\}_2]$ (**2**) at 60° C toluene-d$_8$.

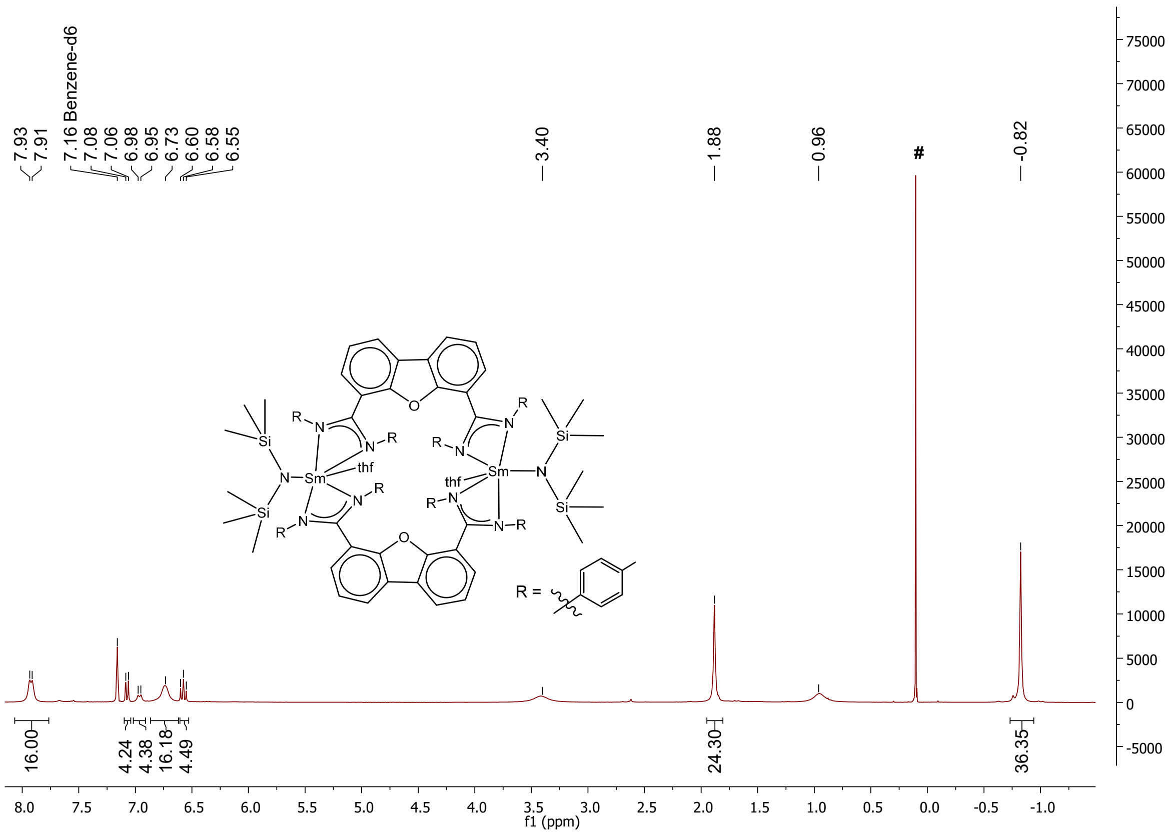

Figure S19. ^{1}H NMR spectrum of $[Sm_2(^{p\text{-Tolyl}}L_{DBF})_2\{N(SiMe_3)_2\}_2(THF)_2]$ (**3**) in C_6D_6, $^{\#}$ $HN(SiMe_3)_2\}_2$.

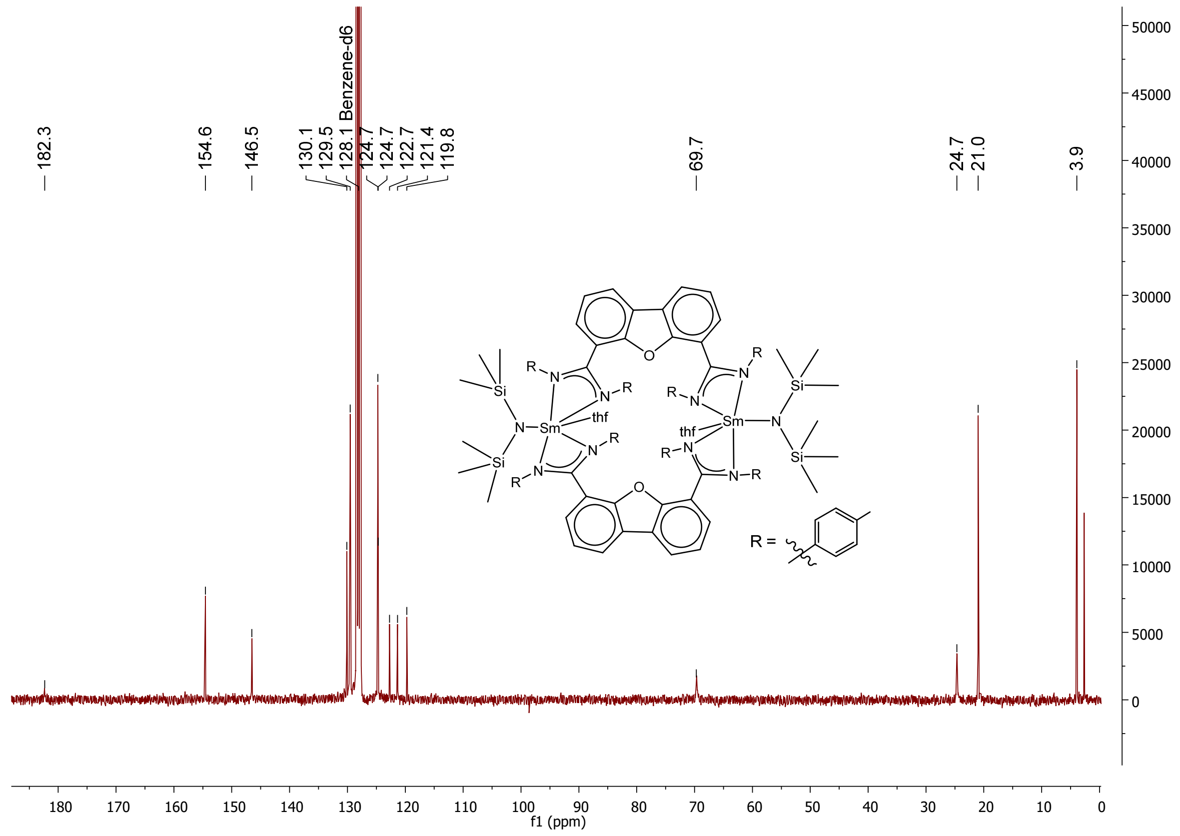

Figure S20. $^{13}C\{^{1}H\}$ NMR spectrum of $[Sm_2(^{p\text{-}Tolyl}L_{DBF})_2\{N(SiMe_3)_2\}_2(THF)_2]$ (**3**) in C_6D_6, # $HN(SiMe_3)_2\}_2$.

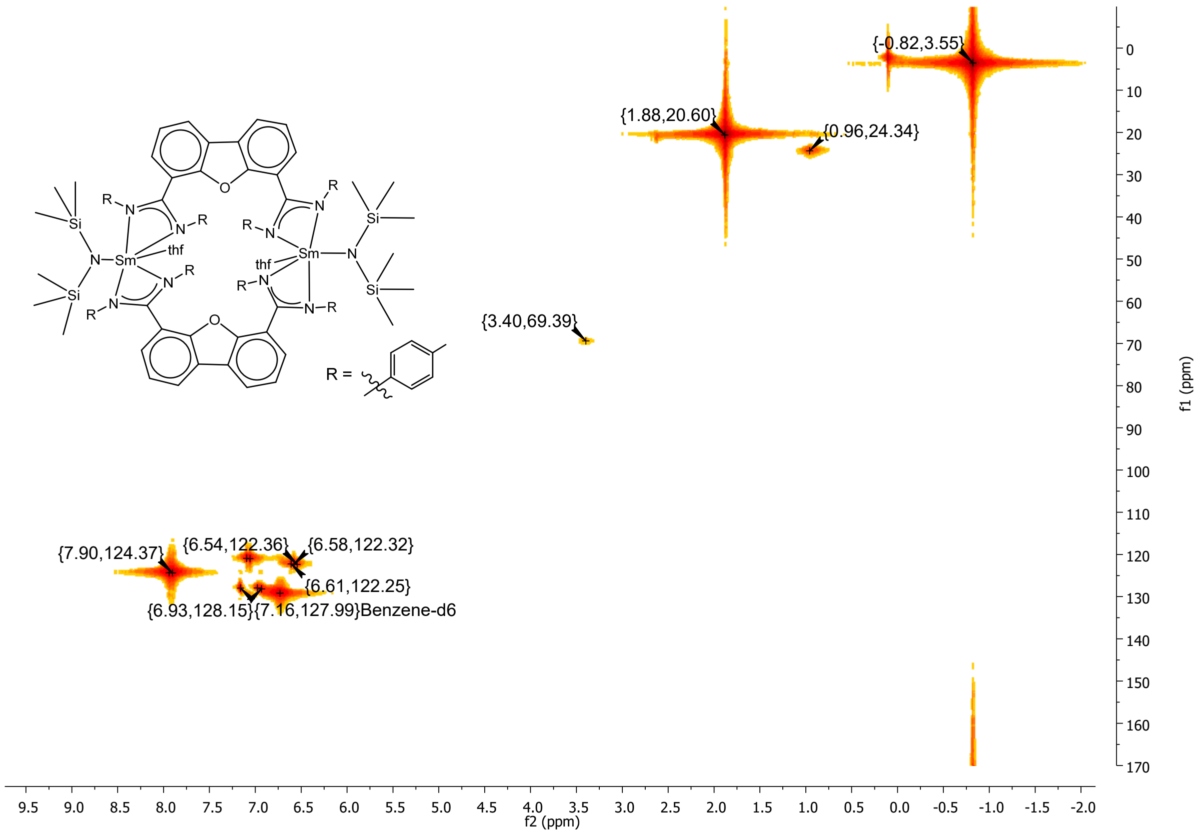

Figure S21. ^{1}H/^{13}C-HMQC NMR spectrum of [$Sm_2(^{p\text{-Tolyl}}L_{DBF})_2\{N(SiMe_3)_2\}_2(THF)_2$] (**3**) in C_6D_6.

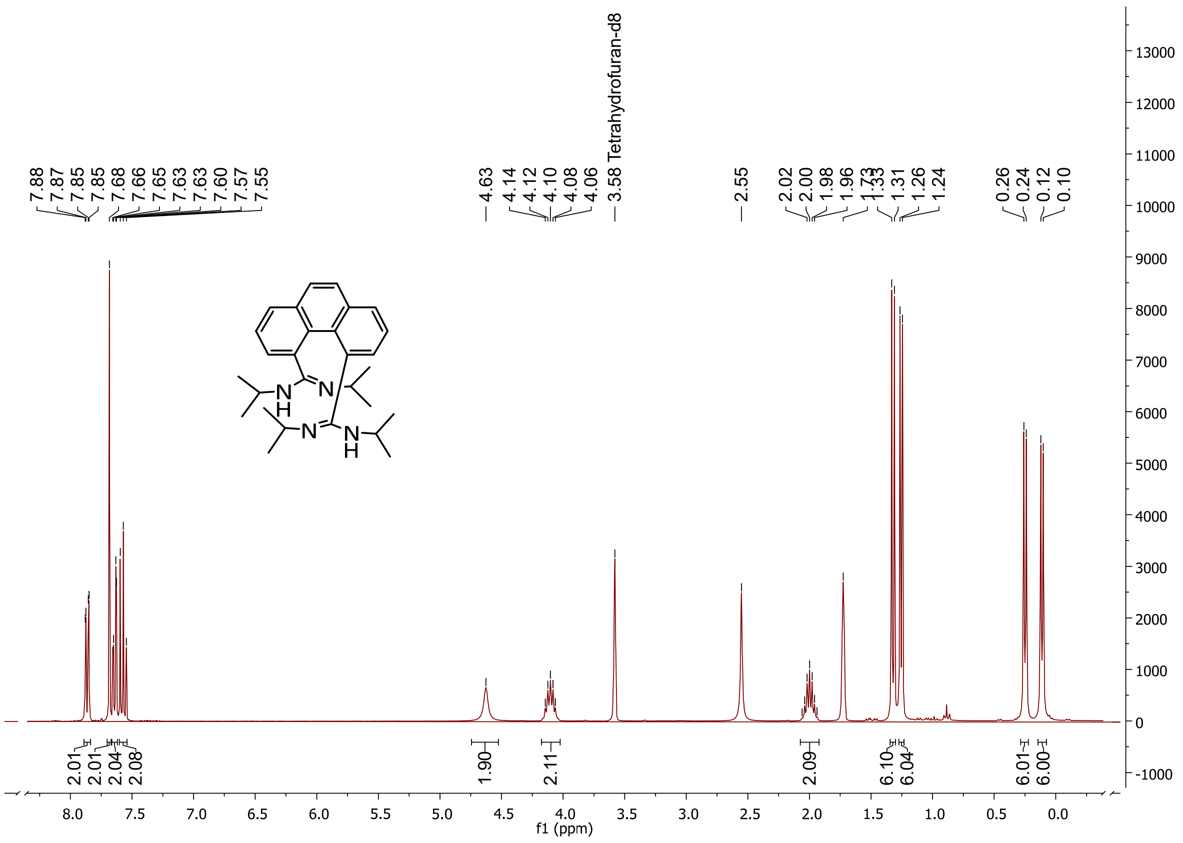

Figure S22. ^{1}H NMR spectrum of $^{iPr}L_{Phen}H_2$ in THF-d$_8$.

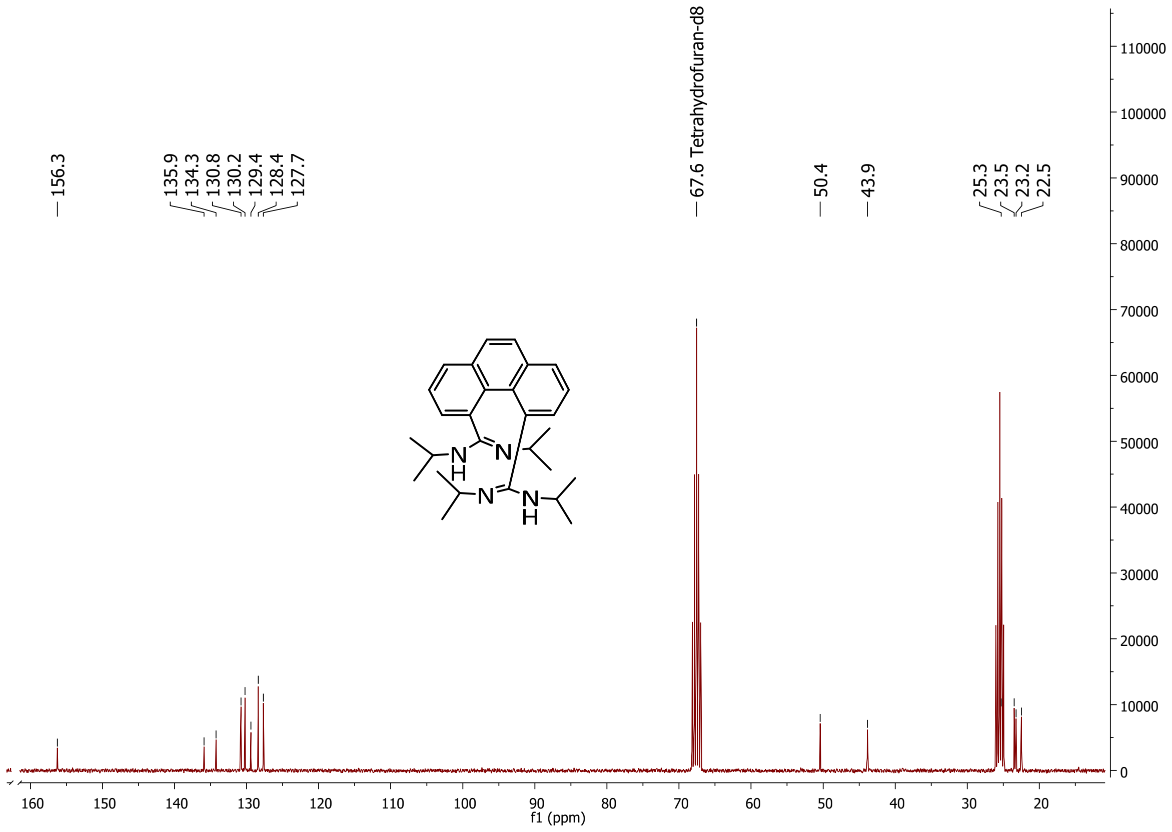

Figure S23. ^{13}C{^{1}H} NMR spectrum of $^{\mathbf{iPr}}\mathbf{L}_{\mathbf{Phen}}\mathbf{H}_2$ in THF-d$_8$.

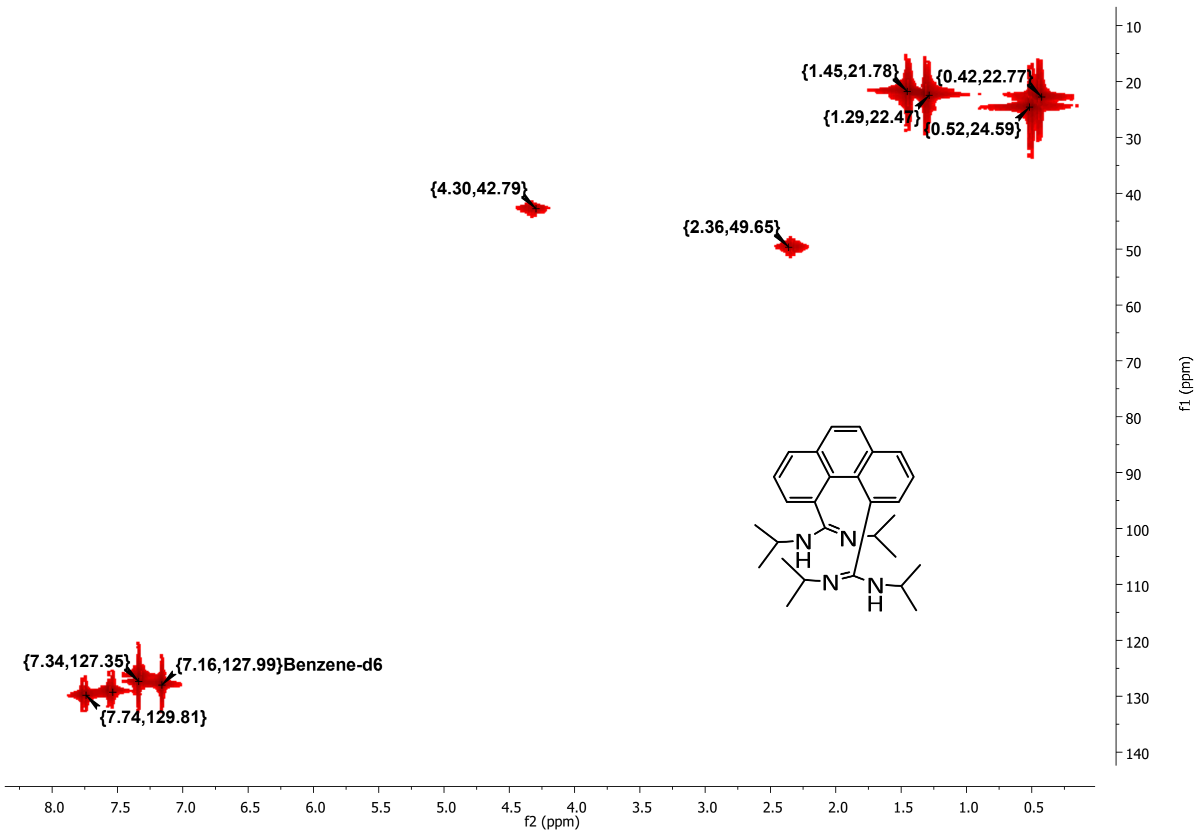

Figure S24. ^{1}H/^{13}C-HMQC NMR spectrum of $^{\mathbf{iPr}}\mathbf{L}_{\mathbf{Phen}}\mathbf{H}_2$ in C_6D_6.

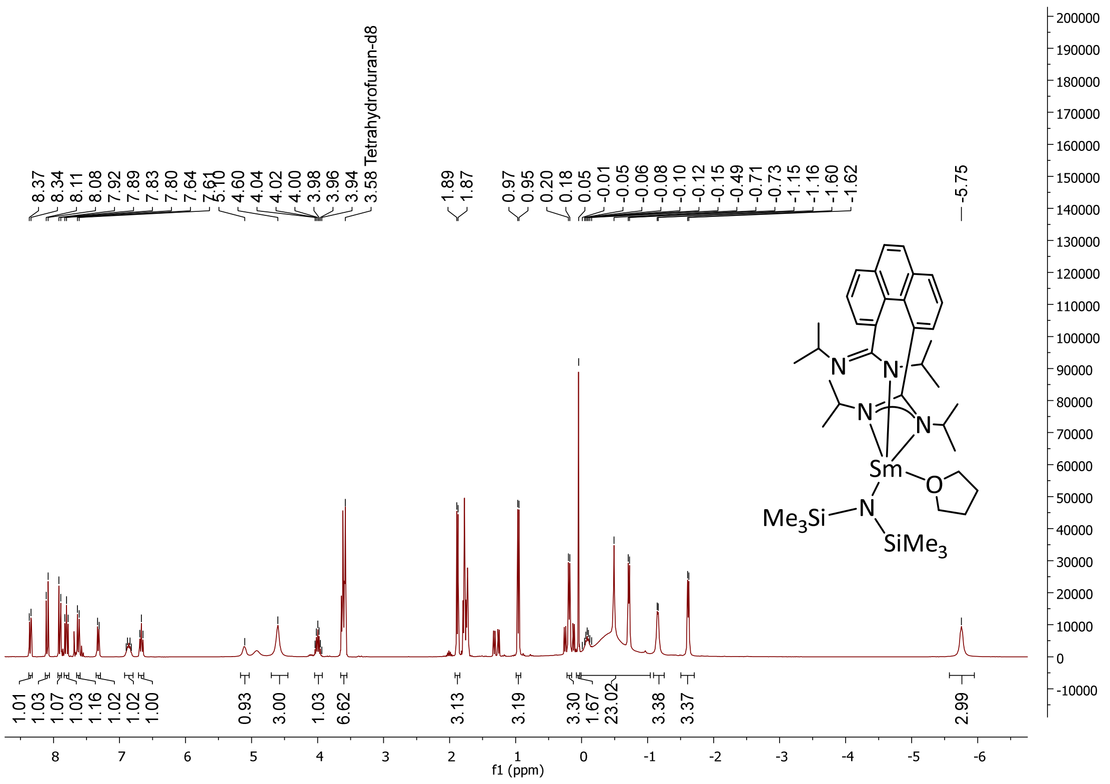

Figure S25. ^{1}H NMR spectrum of [Sm{^{iPr}L$_{Phen}$}(N(SiMe$_3$)$_2$)(thf)] (**4**) in THF-d$_8$.

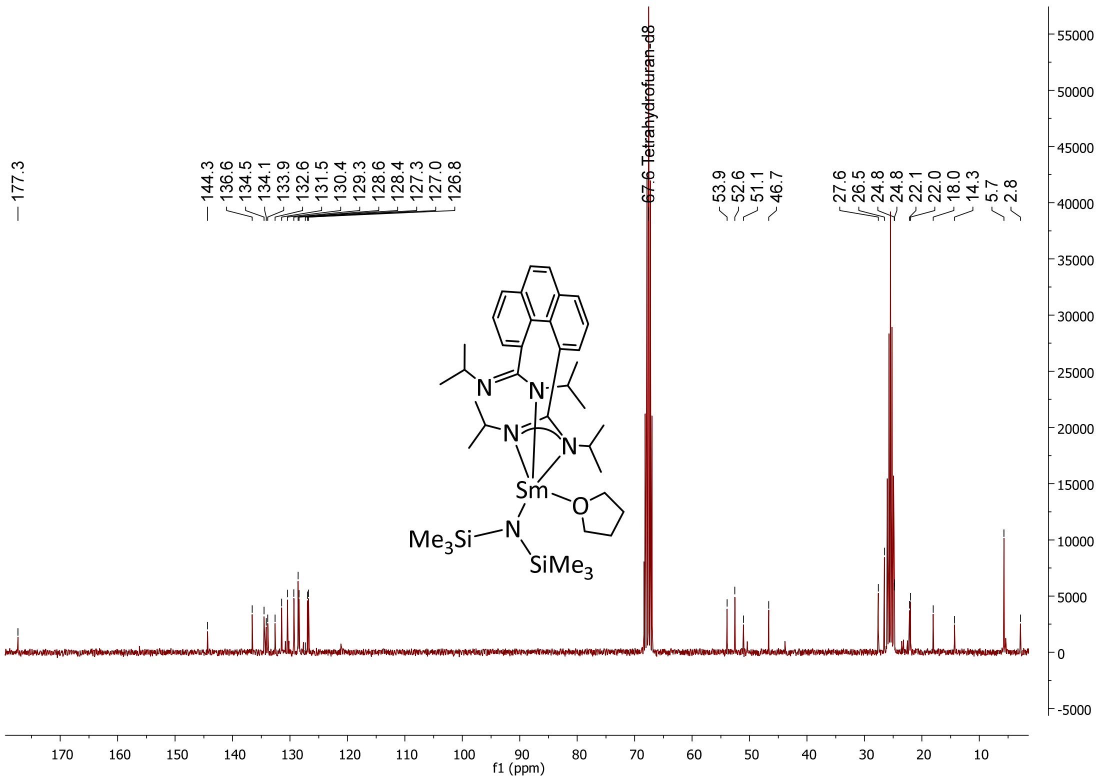

Figure S26. ^{13}C{^{1}H} NMR spectrum of [Sm{^{iPr}L$_{Phen}$}(N(SiMe$_3$)$_2$)(thf)] (**4**) in THF-d$_8$.

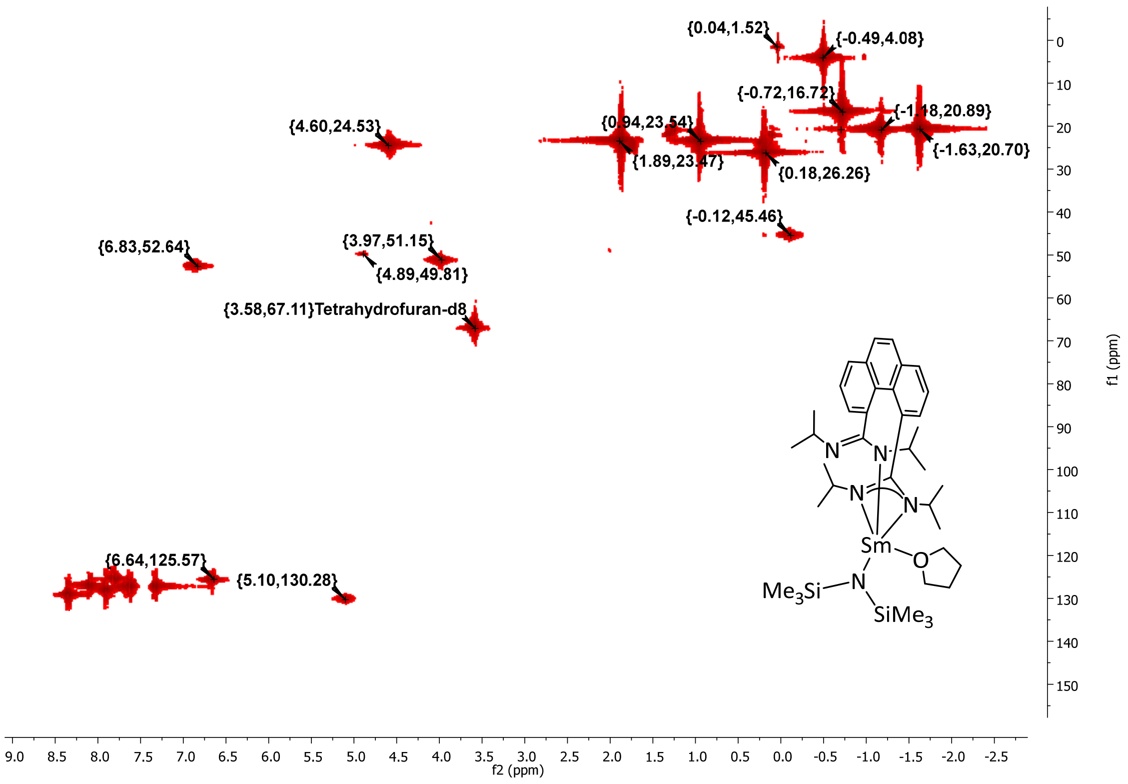

Figure S27. ^{1}H/^{13}C-HMQC NMR spectrum of [Sm{^{iPr}L$_{Phen}$}(N(SiMe$_3$)$_2$)(thf)] (**4**) in THF-d$_8$.

Hydroamination reactions

Procedure:

The catalyst (pure single crystalline material) was weighed into a NMR tube under an argon atmosphere. C_6D_6 (about 0.5 mL) was condensed into the NMR tube and the mixture was frozen at -196 °C. The reactant was injected onto the solid mixture and the whole sample was melted and mixed just before insertion into the core of the NMR machine (t_0). The ratio between the reactant and the product was calculated by comparison of the integrations of the corresponding signals. Ferrocene was used as an internal standard for the kinetic measurements. The substrates 2,2-diphenyl-5-hexenyl-1amine (**1a**),[7] *C*-(1-allyl-cyclohexyl)-methylamine (**1b**),[8] 2,2-dimethylpent-4-en-1-amine (**1c**),[8] 1-amino-2,2-diphenyl-4-methylpent-4-ene (**1d**),[7] and [1-(pent-2-ynyl)-cyclohexyl]methanamine (**1e**)[8] were synthesized according to literature procedures. The ^{1}H NMR data of 2-methyl-5,5-diphenylpiperidine (**2a**),[7] 3-methyl-2-aza-spiro-[4.5]decane (**2b**),[9] 2,5-dimethylpyrrolidine (**2c**),[4] 2,2-dimethyl-4,4-diphenylpyrrolidine (**2d**),[7] and 3-propyl-2-azaspiro [4.5]dec-2-ene (**2e**),[8] agree with those reported in the literature.[7-10]

The reactions are not running without a catalyst under these conditions.[11] Blind experiments were performed for all substrates at 60°C for 3h. No conversion was observed.

Kinetic Measurements

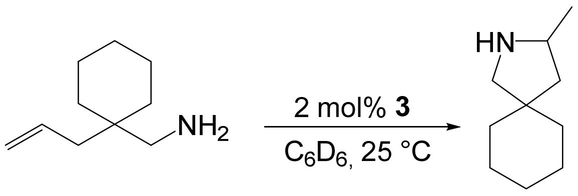

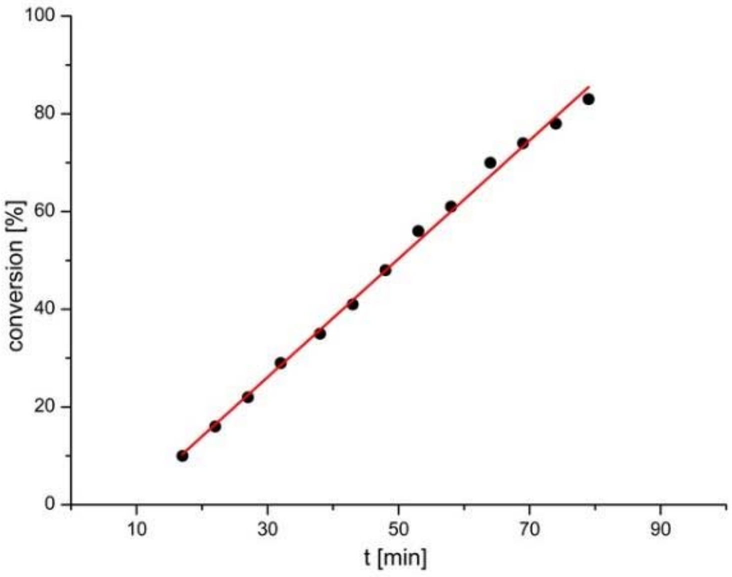

Figure S 28. Reaction of **3** at 25 °C. Zero order with respect to [substrate]. The induction phase (first 15 min.) and the final phase (from about 80 % conversion) were cut off. y = 1.21147x; R^2 = 0.99654; k = 20.19 · 10^{-3} (mol/s).

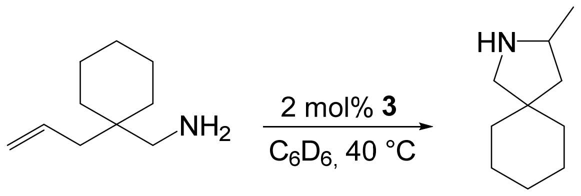

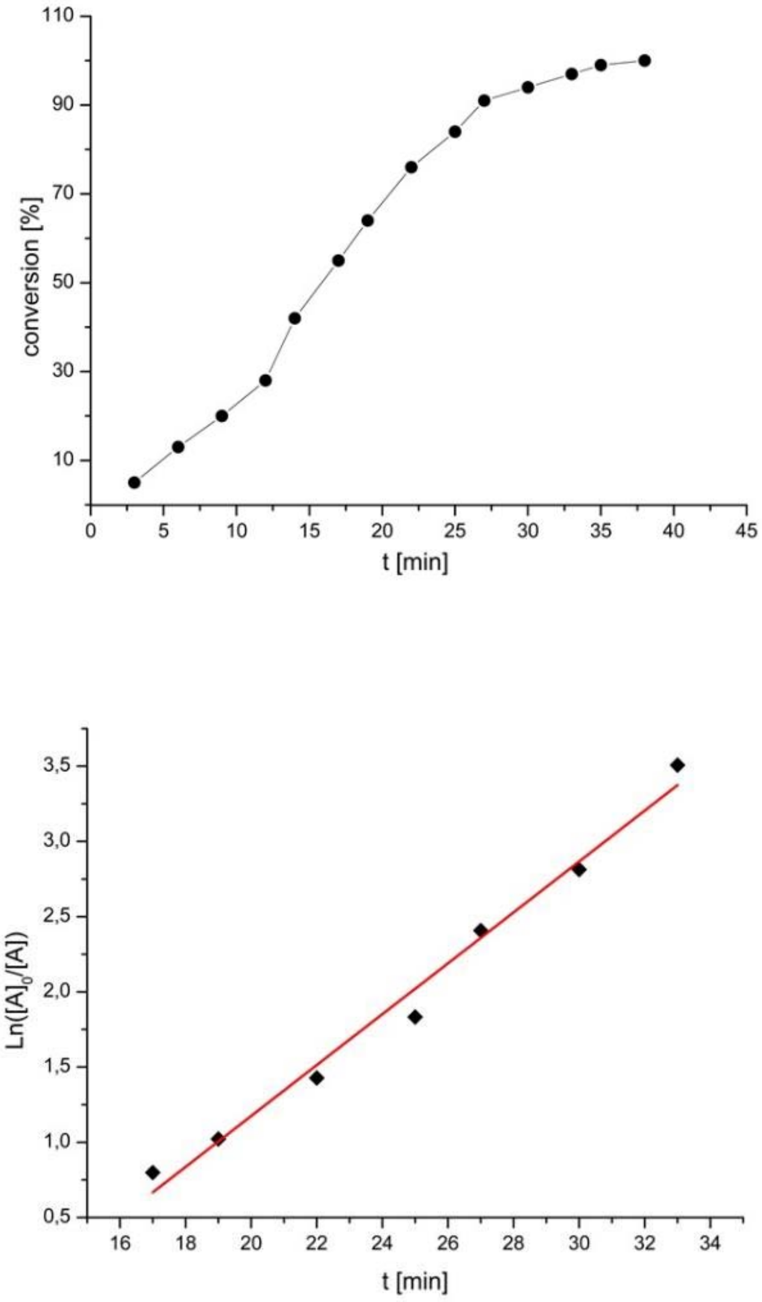

Figure S29. Reaction of **3** at 40 °C. Nearly first order with respect to [substrate] (y = 0.1692x; R^2 = 0.98297; k = 2.82 · 10^{-3} s^{-1}). For the determination of the kinetics, the induction phase (first 5 measurement points (about the first 15 min.) and the final phase (last two points) were cut off.

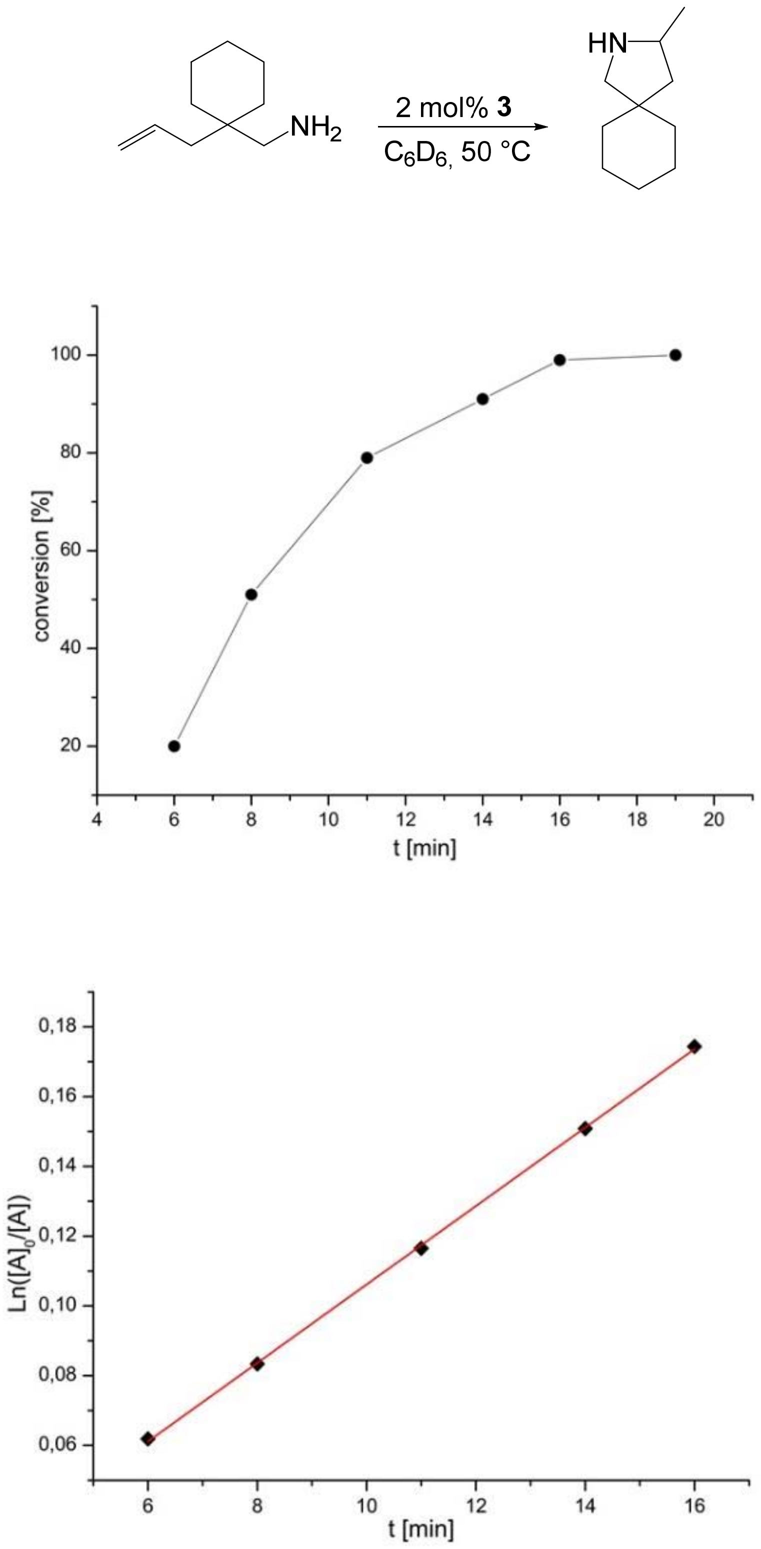

Figure S30: Reaction of **3** at 50 °C. First order with respect to [substrate] ($y = 0.0112x$; $R^2 = 0.9997$; $k = 1.87 \cdot 10^{-3}\ s^{-1}$).

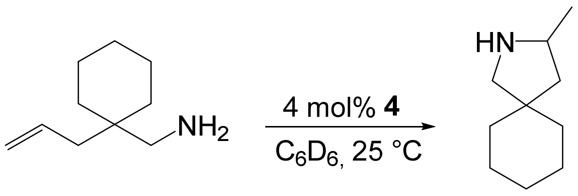

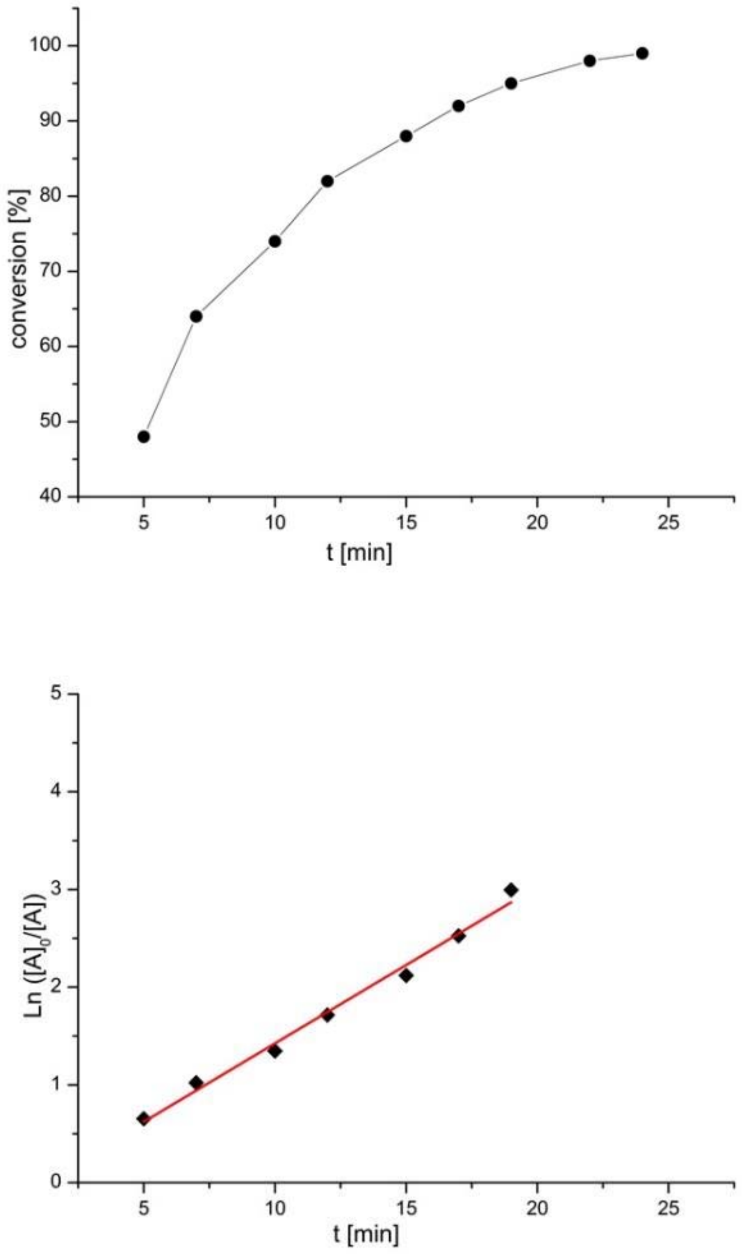

Figure S31. Reaction of **4** at 25 °C. First order with respect to [substrate] (y = 0.16046x; R^2 = 0.98793; k = 2.67 · 10^{-3} $(s)^{-1}$).

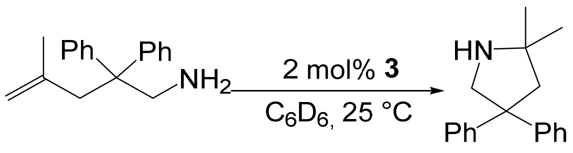

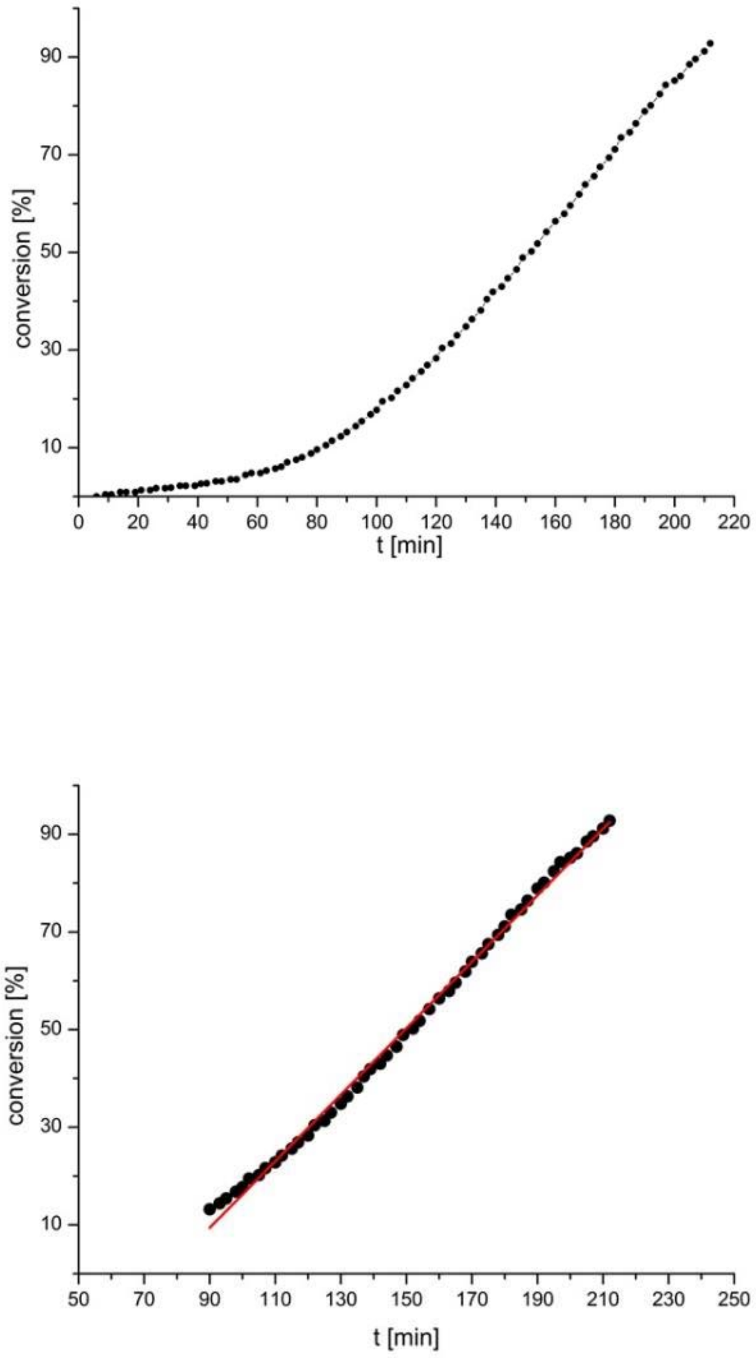

Figure S32. Reaction of **3** at 25 °C. Zero order with respect to [substrate] (y = 0.68101x; R^2 = 0.99681; k = 11.35 · 10^{-3} (mol/s)). For the determination of the kinetics, the induction phase (about the first 90 min.) and the final phase (from about 93 % conversion) were cut off.

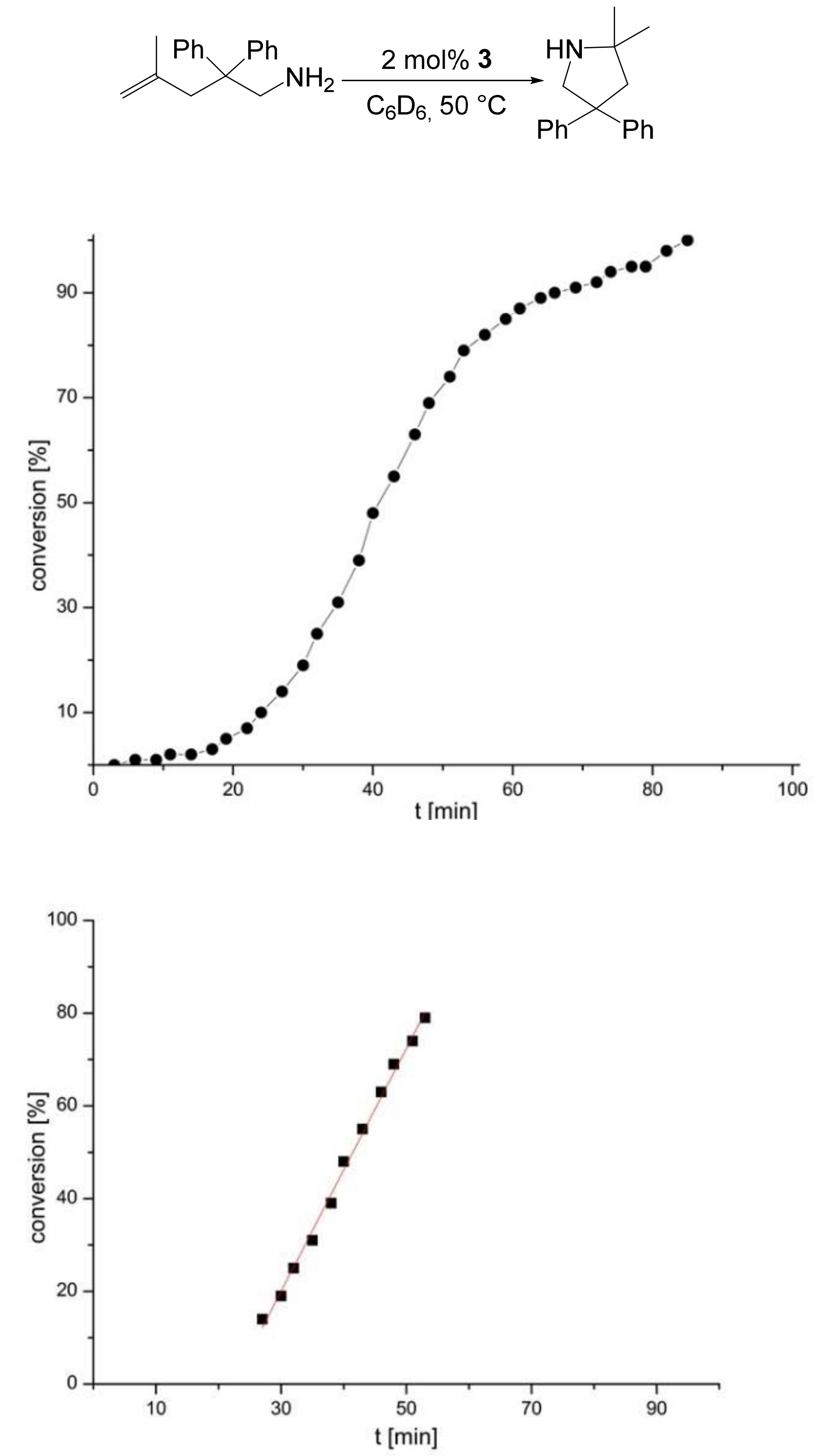

Figure S33. Reaction of **3** at 50 °C. Zero order with respect to [substrate] ($y = 2.61815x$; $R^2 = 0.99489$; $k = 43.63 \cdot 10^{-3}$ (mol/s)). For the determination of the kinetics, the induction phase (about first 25 min.) and the final phase (from about 80 % conversion) were cut off.

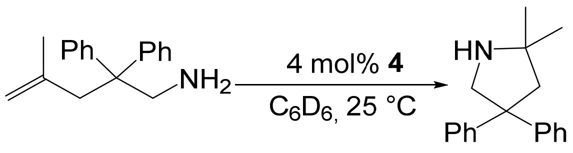

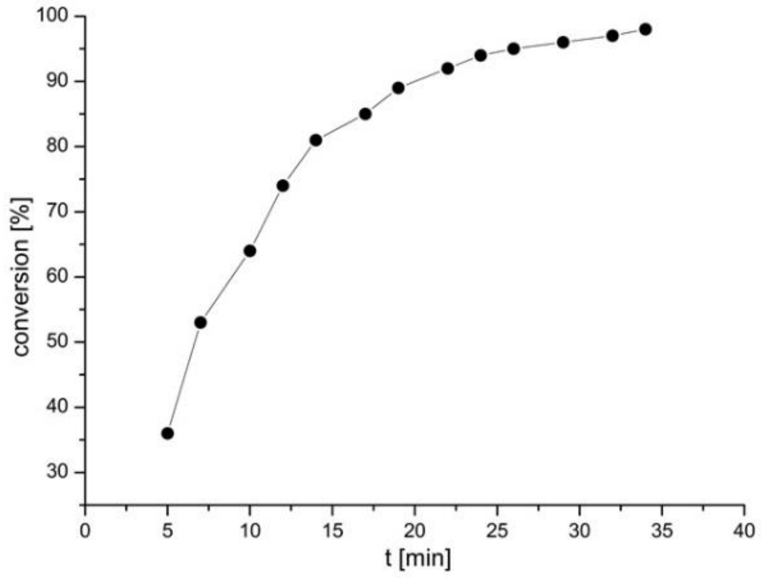

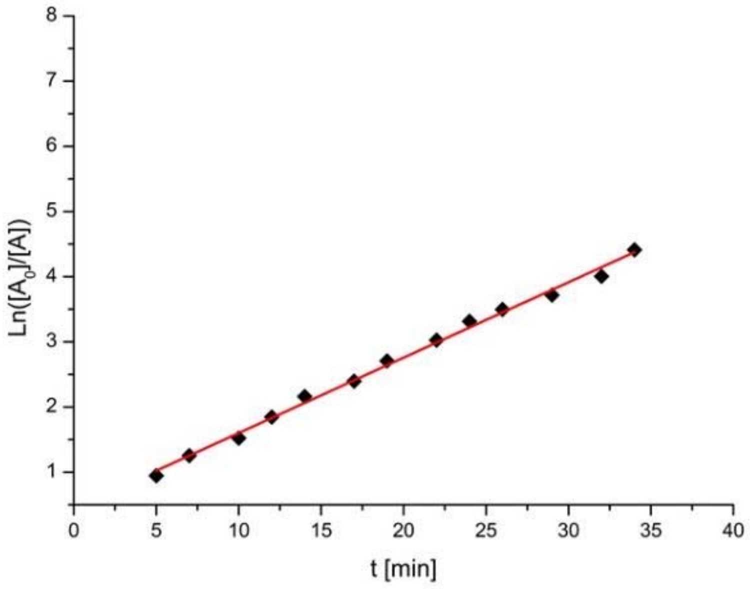

Figure S34. Reaction of **4** at 25 °C. First order kinetics with respect to [substrate] (y = 0.11568x; R^2 = 0.99508; k = 1.93 · 10^{-3} s^{-1}). For the determination of the kinetics, the final phase (from about 99 % conversion) was cut off.

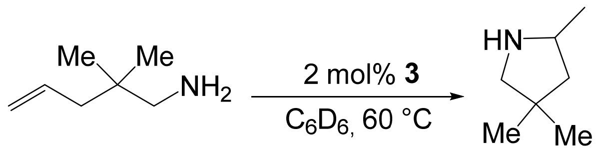

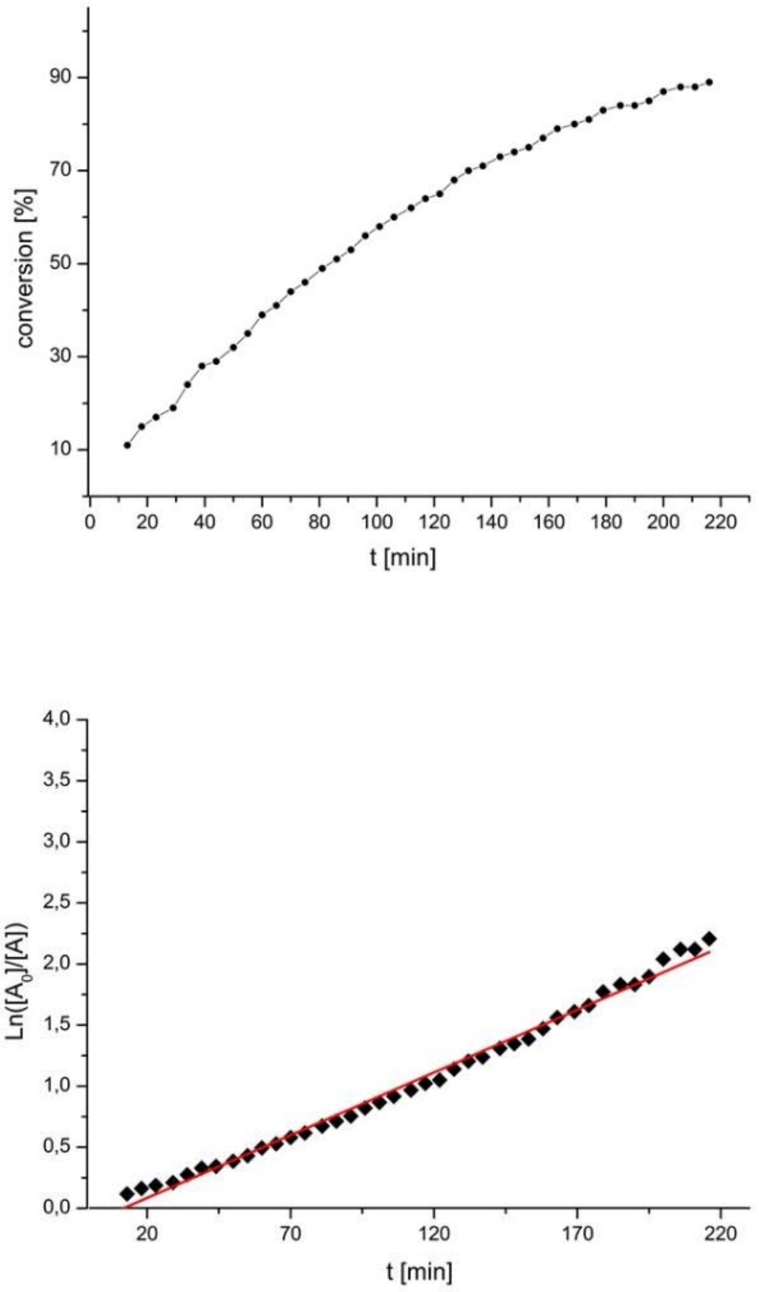

Figure S35. Reaction of **3** at 60 °C. First order kinetics with respect to [substrate] (y = 0.0102x; R^2 = 0.99222; k = 1.7 · 10^{-4} s^{-1})

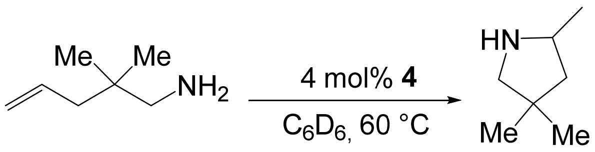

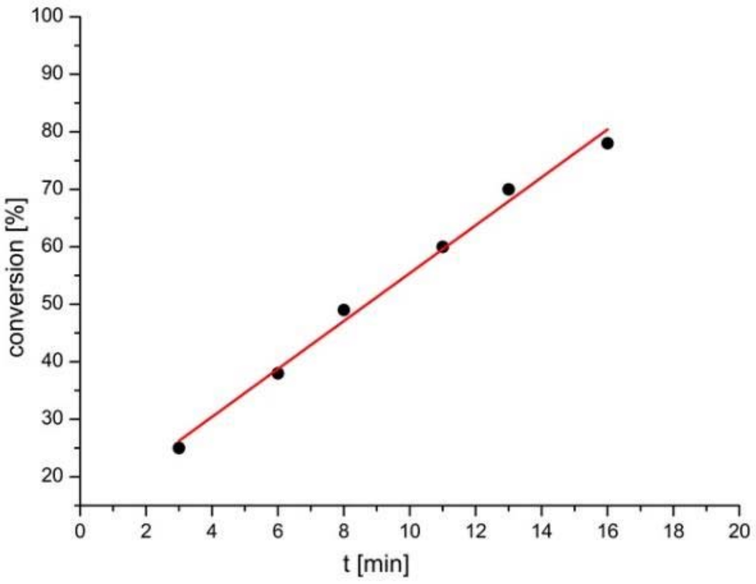

Figure S36. Reaction of **4** at 60 °C. Zero order with respect to [substrate] (y = 4.1674x; R^2 = 0.98984; k = 69.46 · 10^{-3} (mol/s)). For the determination of the kinetic the final phase (from about 78 % conversion (last four points)) was cut off.

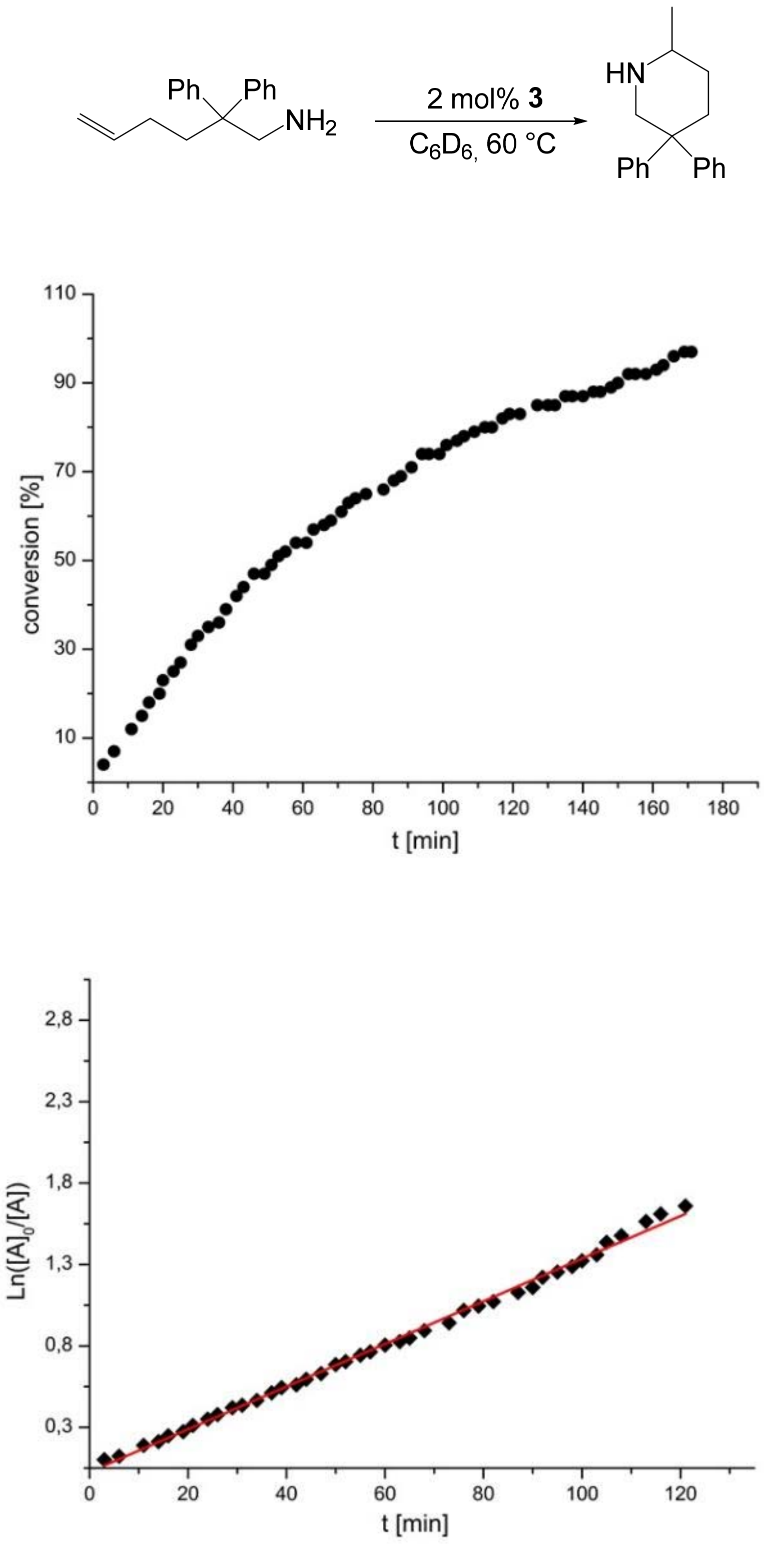

Figure S37. Reaction of **3** at 60 °C. First order with respect to [substrate] (y = 0.013x; R^2 = 0.99676; k = 2.17 · 10^{-4} s^{-1}). For the determination of the kinetics, the final phase (from about 80 % conversion) was cut off.

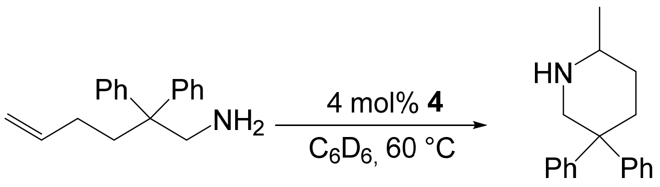

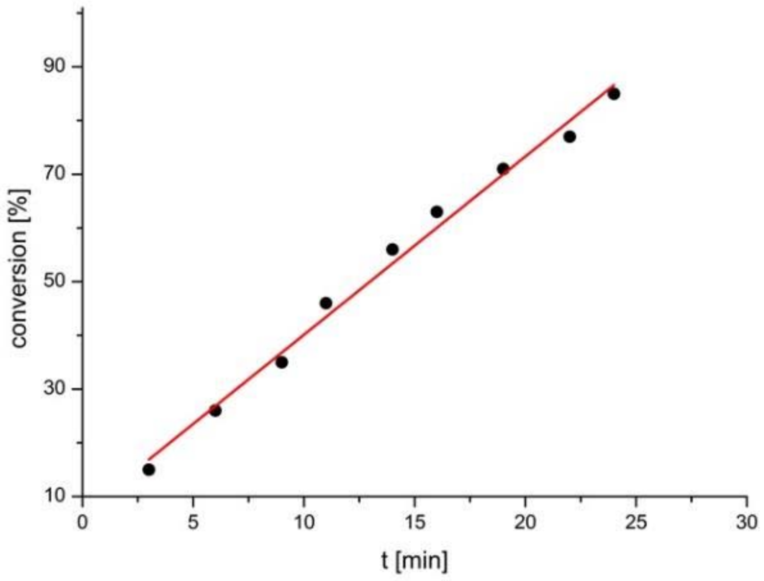

Figure S38. Reaction of **4** at 60 °C. Zero order with respect to [substrate] (y= 3.3199x; R^2 = 0.98955; k = 55.33 · 10^{-3} (mol/s)). For the determination of the kinetics, the final phase (from about 85 % conversion) was cut off.

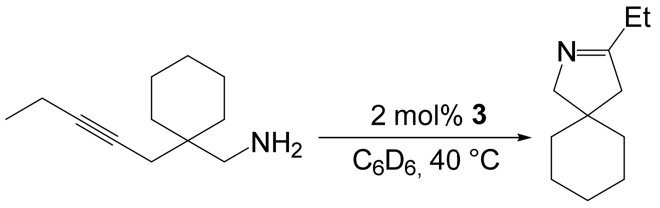

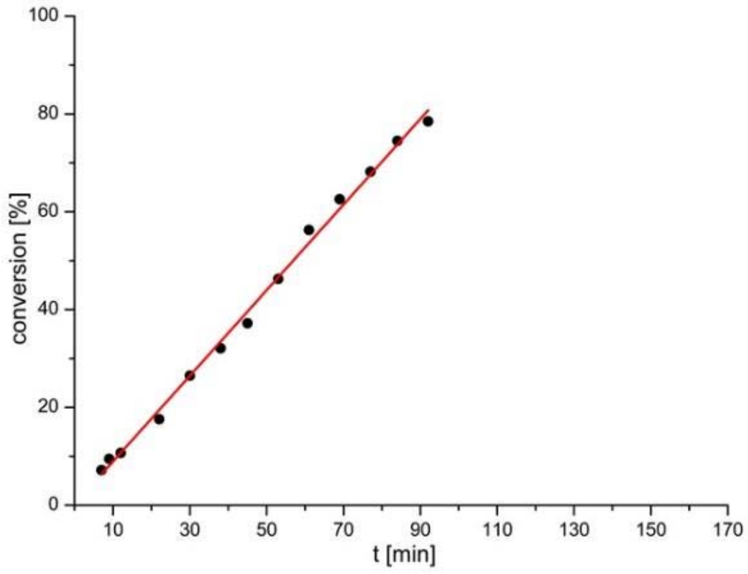

Figure S39. Reaction with **3** at 40 °C. Zero order with respect to [substrate] (y = 0.8753x; R^2 = 0.9957; k = 14.59 $\cdot 10^{-3}$ (mol/s)). For the determination of the kinetics, the final phase (from about 79 % conversion) was cut off.

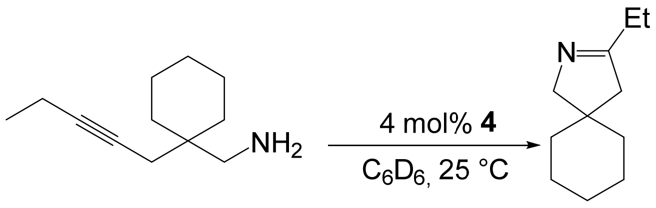

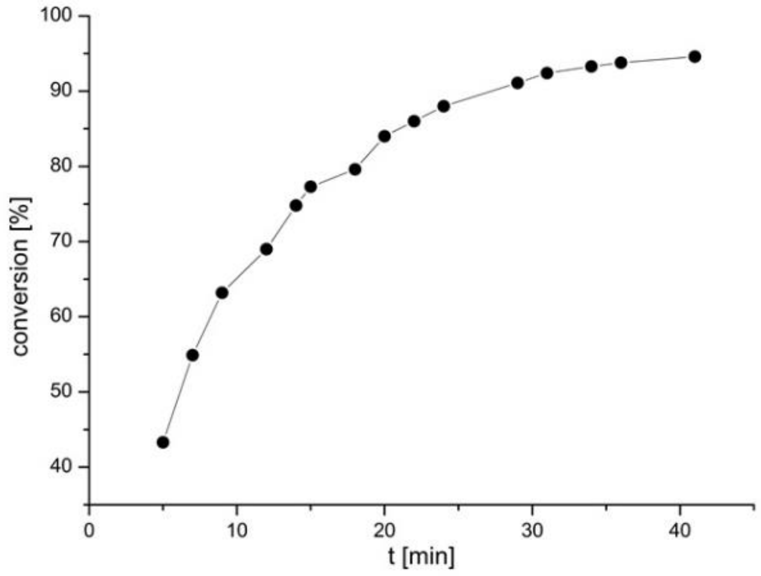

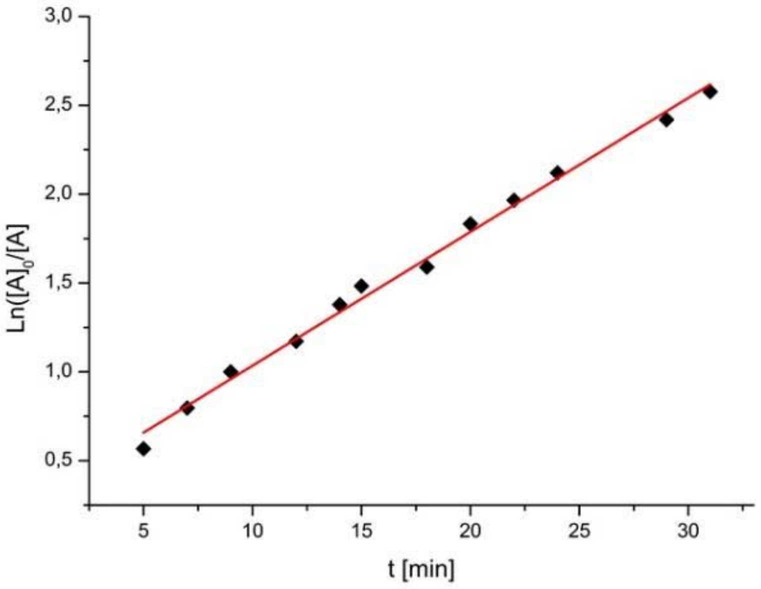

Figure S40. Reaction of **4** at 25 °C. First order with respect to [substrate] (y = 0.0753x ; R^2 = 0.99329; k = 1.26 · 10^{-3} s^{-1}).

NMR Spectra of the Hydroamination Products

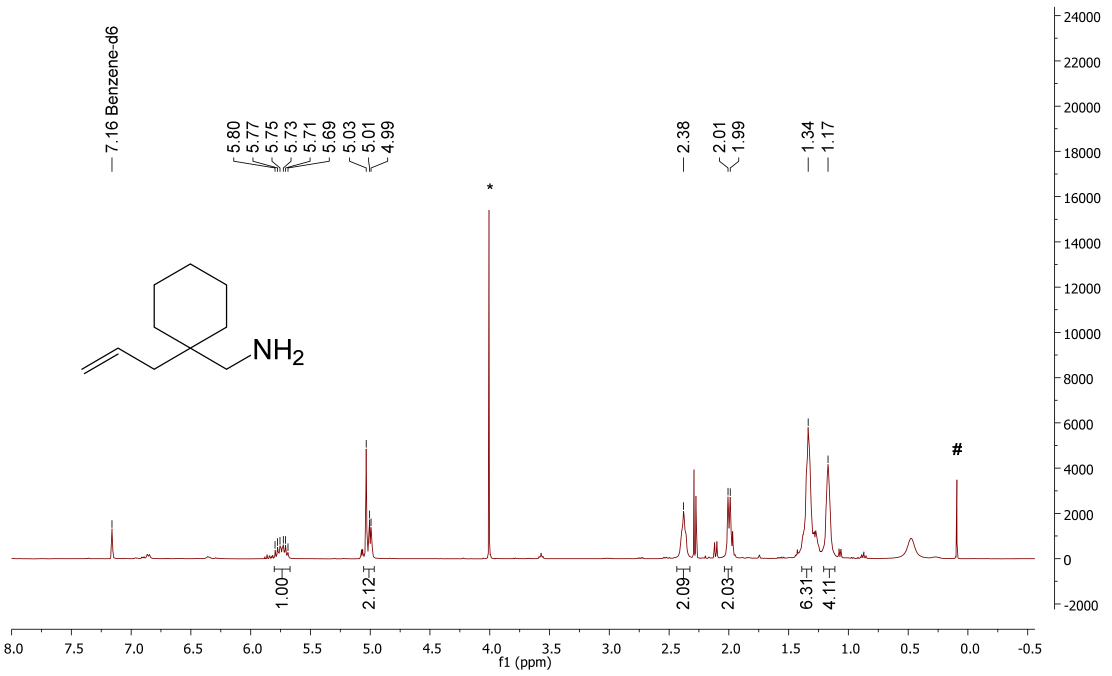

Figure S41: ^{1}H NMR spectrum of *C*-(1-allyl-cyclohexyl)-methylamine using complex **3** as catalyst (Table 1, entry 1). * Ferrocen, # HN(SiMe$_3$)$_2$}$_2$.

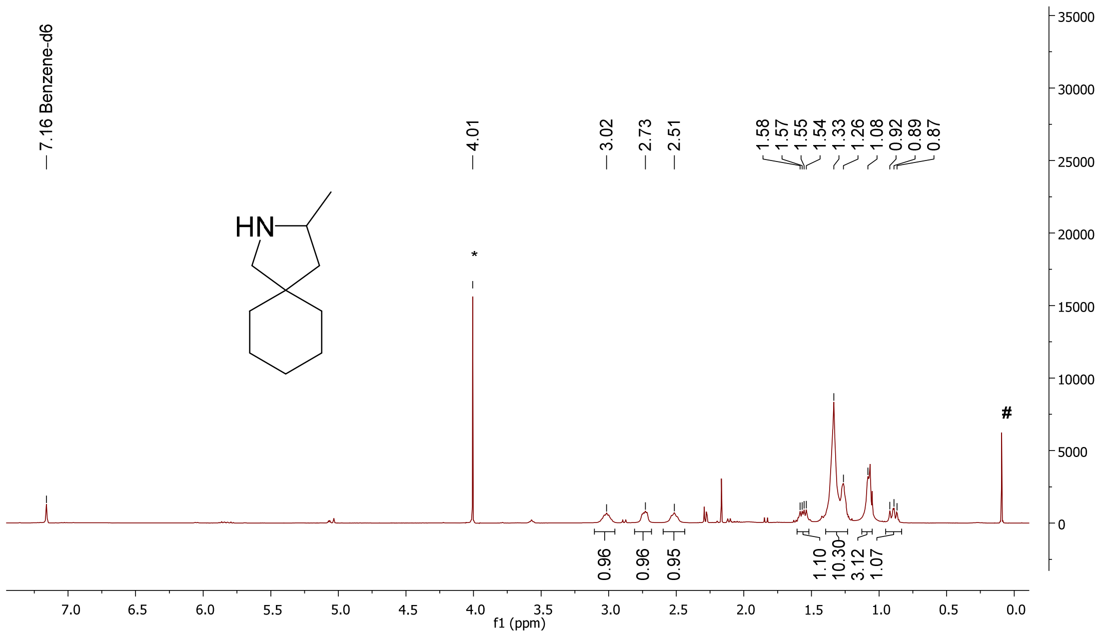

Figure S42: ^{1}H NMR spectrum of 3-methyl-2-aza-spiro-[4.5]decane using complex **3** as catalyst (Table 1, entry 1). * Ferrocen, # HN(SiMe$_3$)$_2$}$_2$.

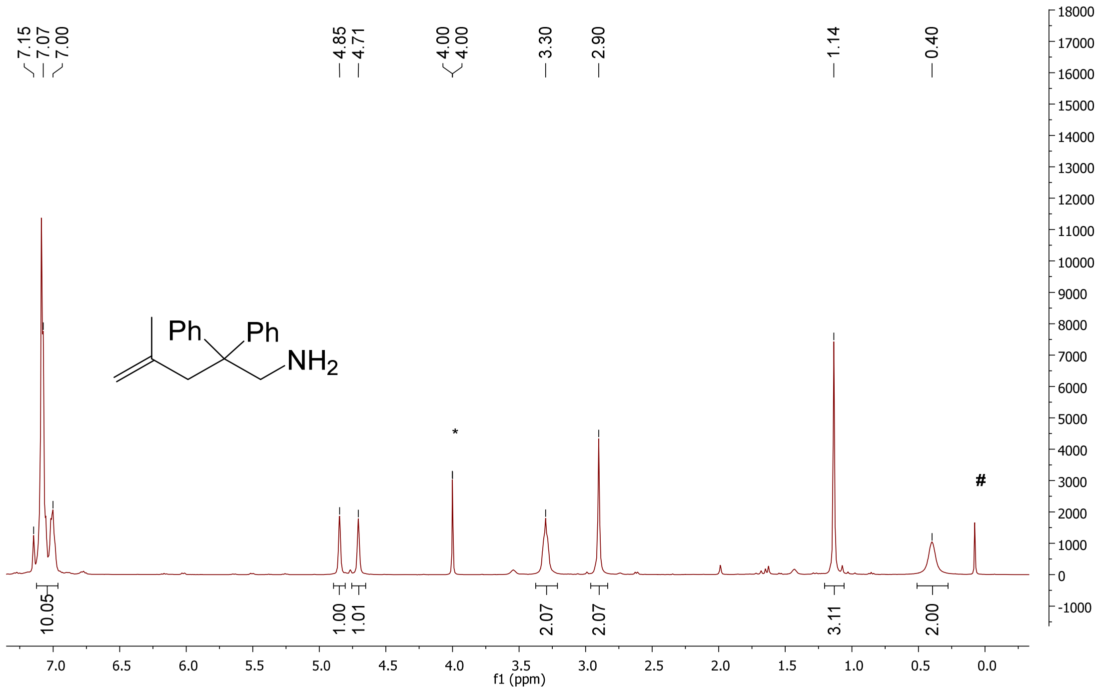

Figure S43: ^{1}H NMR spectrum of 1-amino-2,2-diphenyl-4-methylpent-4-ene using complex **3** as catalyst (Table 1, entry 6). * Ferrocen, # $HN(SiMe_3)_2\}_2$.

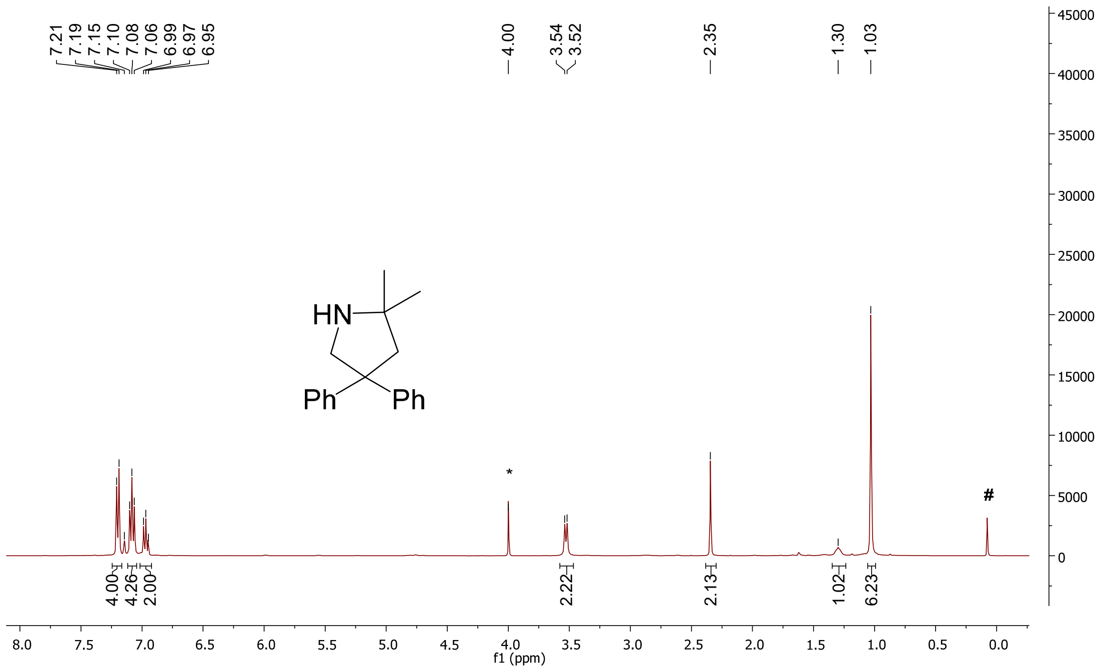

Figure S44: ^{1}H NMR spectrum of 2,2-dimethyl-4,4-diphenylpyrrolidine using complex **3** as catalyst (Table 1, entry 6). * Ferrocen, # $HN(SiMe_3)_2\}_2$.

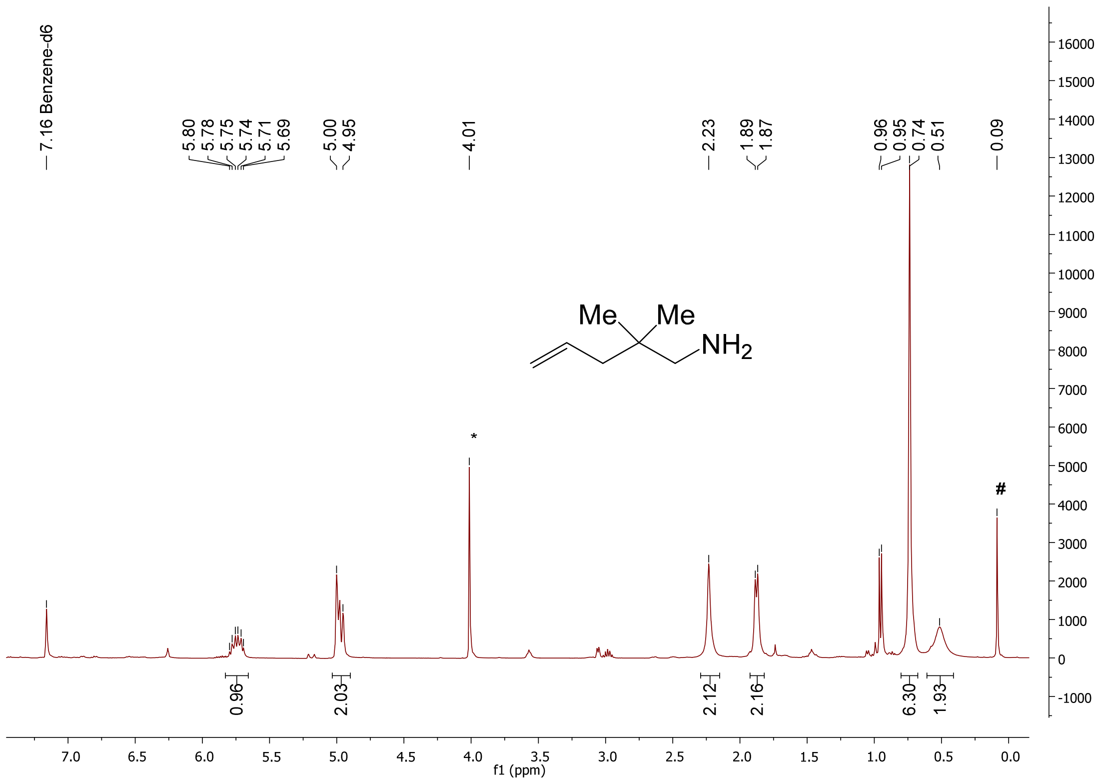

Figure S45: ^{1}H NMR spectrum of 2,2-dimethylpent-4-en-1-amine using complex **3** as catalyst (Table 1, entry 9). * Ferrocen, $^{\#}$ HN(SiMe$_3$)$_2$}$_2$.

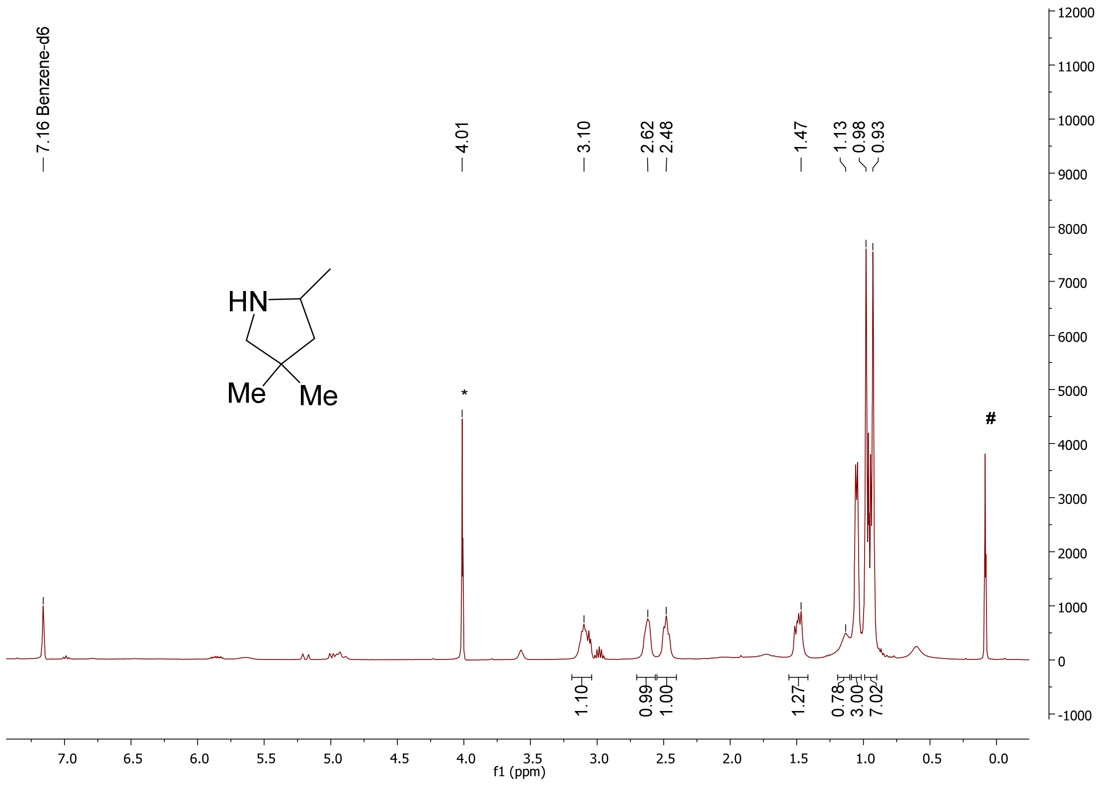

Figure S46: ^{1}H NMR spectrum of 2,5-dimethylpyrrolidine using complex **3** as catalyst (Table 1, entry 9). * Ferrocen, $^{\#}$ HN(SiMe$_3$)$_2$}$_2$.

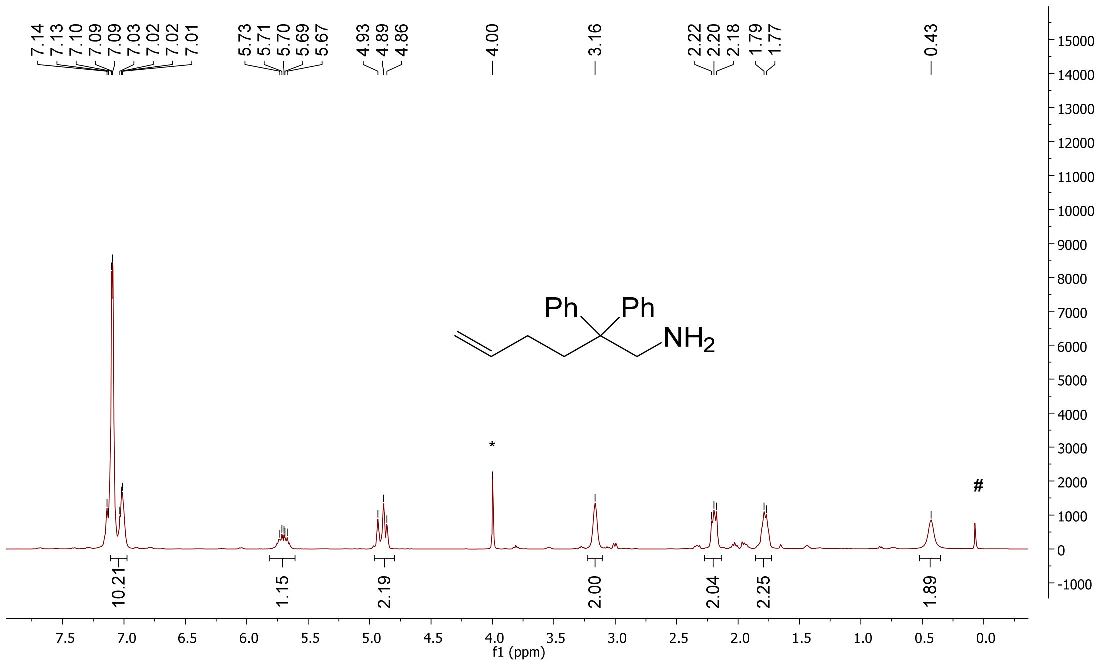

Figure S47: ^{1}H NMR spectrum of 2,2-diphenyl-5-hexenyl-1amine using complex **3** as catalyst (Table 1, entry 11). * Ferrocen, $^{\#}$ $HN(SiMe_3)_2\}_2$.

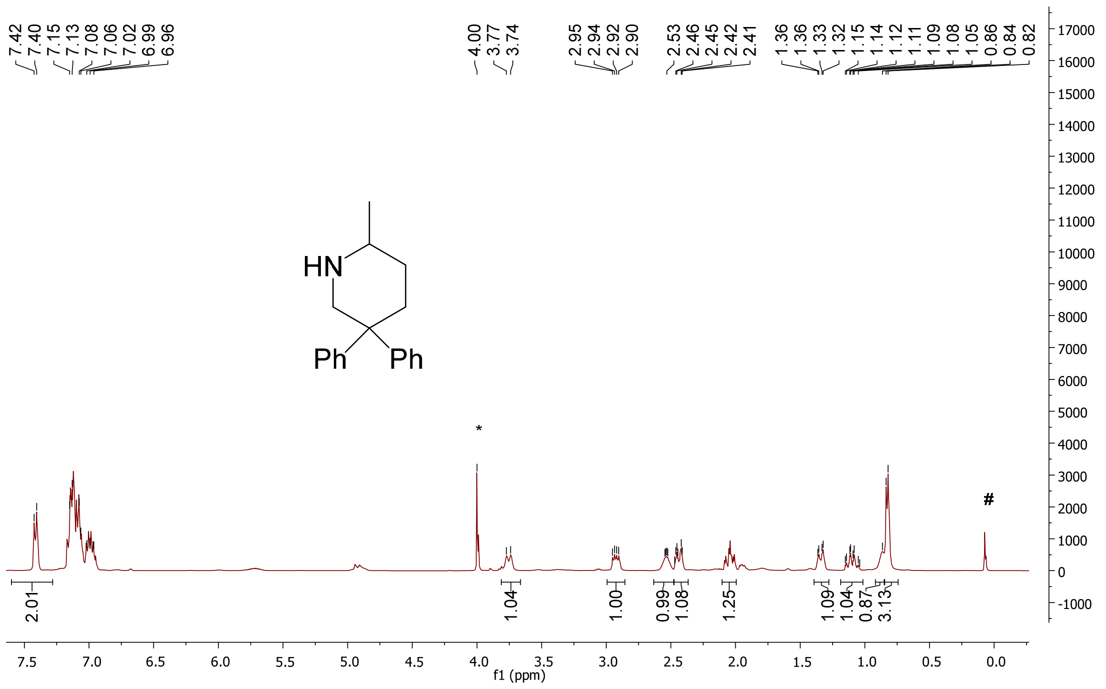

Figure S48: ^{1}H NMR spectrum of 2-methyl-5,5-diphenylpiperidine using complex **3** as catalyst (Table 1, entry 11). * Ferrocen, $^{\#}$ $HN(SiMe_3)_2\}_2$.

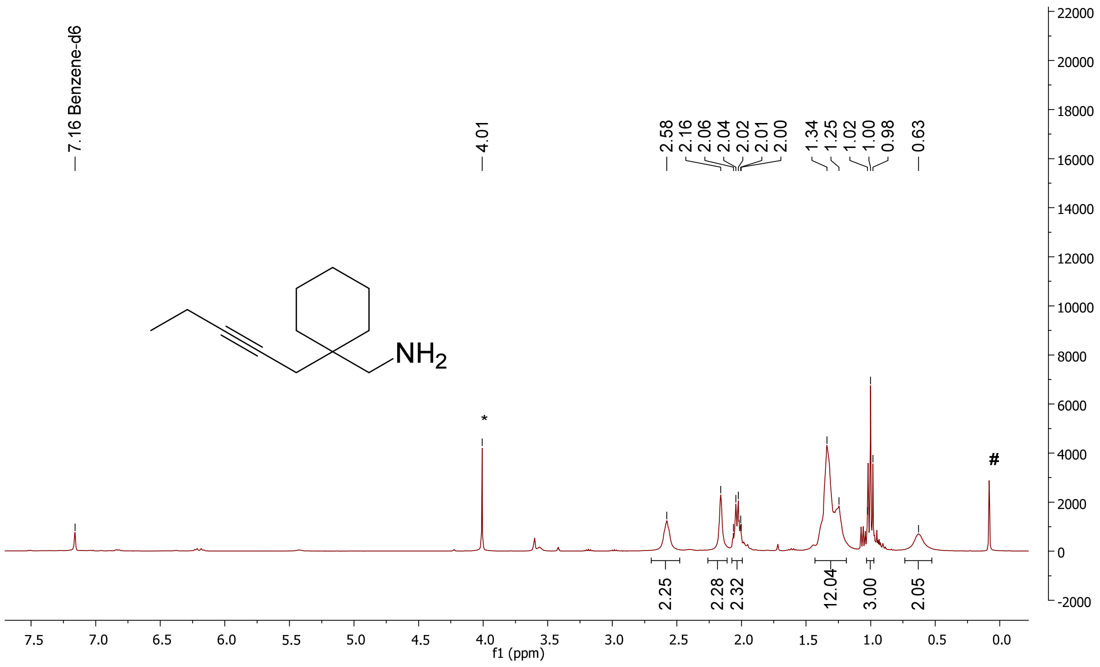

Figure S49: ^{1}H NMR spectrum of [1-(pent-2-ynyl)-cyclohexyl]methanamine using complex **3** as catalyst (Table 1, entry 14). * Ferrocen, # HN(SiMe$_3$)$_2$}$_2$.

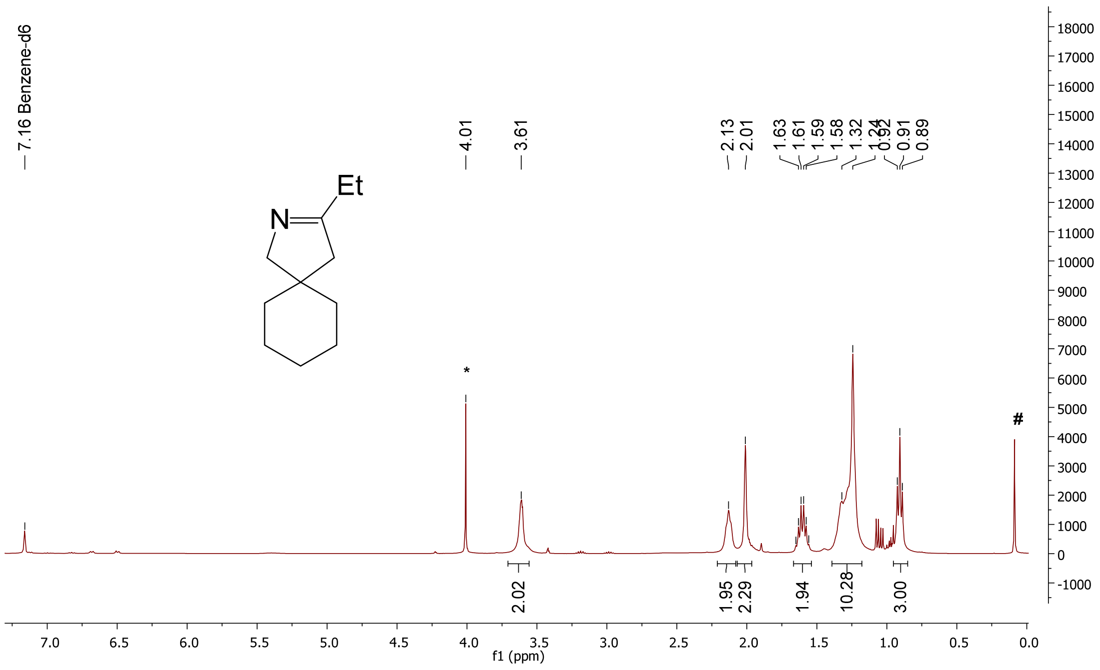

Figure S50: ^{1}H NMR spectrum of 3-propyl-2-azaspiro [4.5]dec-2-ene using complex **3** as catalyst (Table 1, entry 14). * Ferrocen, # HN(SiMe$_3$)$_2$}$_2$.

References

1. D. C. Bradley, J. S. Ghotra and F. A. Hart, *J. Chem. Soc., Dalton Trans.*, 1973, 1021.
2. G. M. Sheldrick, *Acta Crystallogr., Sect. A* 2008, **64**, 112.
3. *Stoe & Cie X-RED*, Darmstadt, Germany, 2002.
4. *Stoe & Cie X-Shape*, Darmstadt, Germany, 2002.
5. *Stoe & Cie GmbH, X-AREA 1.75.*, Darmstadt, Germany, 2015.
6. A. L. Spek, *Acta Crystallogr. Sect. C*, 2015, **71**, 9.
7. M. R. Crimmin, M. Arrowsmith, A. G. M. Barrett, I. J. Casely, M. S. Hill and P. A. Procopiou, *J. Am. Chem. Soc.*, 2009, **131**, 9670.
8. M. Rastätter, A. Zulys and P. W. Roesky, *Chem. Eur. J.*, 2007, **13**, 3606.
9. J.-S. Ryu, G. Y. Li and T. J. Marks, *J. Am. Chem. Soc.*, 2003, **125**, 12584.
10. M. R. Gagne, C. L. Stern and T. J. Marks, *J. Am. Chem. Soc.*, 1992, **114**, 275.
11. (a) P. W. Roesky and T. E. Müller, *Angew. Chem. Int. Ed.*, 2003, **42**, 2708; (b) S. Hong and T. J. Marks, *Acc. Chem. Res.*, 2004, **37**, 673; (c) R. Severin and S. Doye, *Chem. Soc. Rev.*, 2007, **36**, 1407; (d) T. E. Müller, K. C. Hultzsch, M. Yus, F. Foubelo and M. Tada, *Chem. Rev.*, 2008, **108**, 3795; (e) T. Li, J. Jenter and P. W. Roesky, *Struct. Bond.*, 2010, **137**, 165; (f) A. L. Reznichenko and K. C. Hultzsch, in *Chiral Amine Synthesis*, Wiley-VCH Verlag GmbH & Co. KGaA, 2010, pp. 341; (g) J. Hannedouche and E. Schulz, *Chem. Eur. J.*, 2013, **19**, 4972; (h) M. R. Bürgstein, H. Berberich and P. W. Roesky, *Chem. Eur. J.*, 2001, **7**, 3078; (i) A. Zulys, T. K. Panda, M. T. Gamer and P. W. Roesky, *Chem. Commun.*, 2004, 2584.